

## LEVEL CROSSING FOR HOT SPHALERONS

*J. Ambjørn<sup>1</sup>, K. Farakos<sup>2</sup>, S. Hands<sup>3</sup>, G. Koutsoumbas<sup>2</sup> and G. Thorleifsson<sup>1</sup>*

### Abstract

We study the spectrum of the Dirac Hamiltonian in the presence of high temperature sphaleron-like fluctuations of the electroweak gauge and Higgs fields, relevant for the conditions prevailing in the early universe. The fluctuations are created by numerical lattice simulations. It is shown that a change in Chern-Simons number by one unit is accompanied by eigenvalues crossing zero and a change of sign of the generalized chirality  $\tilde{\Gamma}_5 = (-1)^{2T+1}\gamma_5$  which labels these modes. This provides further evidence that the sphaleron-like configurations observed in lattice simulations may be viewed as representing continuum configurations.

---

<sup>1</sup>The Niels Bohr Institute, Blegdamsvej 17, DK-2100 Copenhagen Ø, Denmark

<sup>2</sup>National Technical University of Athens, Department of Physics, GR 157 80, Athens, Greece.

<sup>3</sup>Department of Physics, University of Wales, Swansea, Singleton Park, Swansea SA2 8PP, U.K.

# 1 Introduction

The baryonic current is anomalous in the electroweak theory [1]. This leads to a non-conservation of baryon- and lepton-number. It is of little importance in the present day universe where the processes which violate baryon- and lepton-number conservation are exponentially suppressed. There is evidence that this suppression is not present at the high temperatures prevailing in the early universe [2], and it has played an increasing role in attempts to explain the baryon asymmetry observed in the universe today.

Unfortunately almost any interesting question related to the high temperature phase of the electroweak theory is difficult to address by analytical tools, due to the infrared singularities of the associated high temperature perturbation theory. A generic non-perturbative way to study the high temperature fluctuations of the gauge and Higgs fields is by means of lattice simulations. If we want to address questions related to the anomaly we encounter the difficulty that topology is involved, an inherent continuum concept, and it is important to verify that configurations generated on the lattice during the simulations will qualify as representatives of continuum configurations.

In [2] a real time evolution of classical gauge and Higgs fields was used as an approximation to the high temperature fluctuations present in the electroweak theory in the early universe. The baryon number violation was studied by observing the change in the Chern-Simons number during the time evolution. Since the temperature fluctuations are not small in these simulations it is important to ask if these fluctuations might spoil the picture of level crossing, which somehow is the justification of viewing the change in Chern-Simons number as responsible for a change in fermion number.

In [3] it was shown that the gauge field fluctuations which lead to a change in Chern-Simons numbers at the same time cause the lowest eigenvalue of the *massless* Dirac Hamiltonian to cross zero, in agreement with the level crossing picture where such a crossing results in the conversion of particles to anti-particles (or vice versa). In addition the measurement of the spatial extension of energy lumps associated with the fluctuations corroborated the interpretation of these as representing continuum physics. However, in the full electroweak theory an important ingredient is the Higgs field. It couples to the fermions and is responsible for particle masses in the broken phase. At first sight it is maybe surprising that the level crossing picture is still true in this case since the eigenstates of the full Dirac Hamiltonian are massive when one includes the coupling to the Higgs field. This is in particular true if we consider the ground state configuration in the broken phase :  $\phi = \phi_0$ ,

$A_\mu = 0$ . The situation is different in the presence of a sphaleron. For a sphaleron configuration there is precisely one normalizable eigenmode and it has zero energy [4, 5]. As a consequence a gauge-Higgs configuration which changes continuously from one vacuum configuration to a neighboring one, passing through a sphaleron configuration on the way, will trigger an adiabatic change of the lowest positive eigenvalue such that it passes through zero and ends up as the “highest” negative eigenvalue [5].

In many ways the situation around a sphaleron configuration is similar to the situation around the simplest non-abelian monopole. In that case there exists an index theorem for open three-dimensional space [6] which tells us that the difference  $n$  between the number of normalizable eigenfunctions of positive chirality and the normalizable eigenfunctions of negative chirality, of the Dirac Hamiltonian with eigenvalue zero, is related to the charge of the monopole  $Q$  by

$$Q = \frac{4\pi n}{e}. \quad (1)$$

$n$  can be expressed in terms of the Higgs field:

$$n = \frac{1}{4\pi} \int_{S_\infty} d^2x_i \varepsilon_{ijk} \varepsilon^{abc} \tilde{\phi}^a \partial_j \tilde{\phi}^b \partial_k \tilde{\phi}^c, \quad (2)$$

where  $\tilde{\phi}^a = \phi^a/|\phi|$  for a Higgs field in the adjoint representation. Eq. (2) reflects that  $|\phi|$  is assumed to be different from zero at spatial infinity and consequently that the map  $x \in S_\infty^2 \rightarrow \tilde{\phi}(x) \in S^2$  has winding number  $n$ . In the case of the sphaleron we do not have a similar topological interpretation since the Higgs field is a complex doublet, i.e. it has four real components and we will have a map  $x \in S_\infty^2 \rightarrow \tilde{\phi}(x) \in S^3$ . This map is always contractable to the trivial map ( $\pi_2(S^3) = 0$ ). However, for a continuous family of static fields  $\phi(x; \tau), A_i(x; \tau)$ ,  $\tau \in [0, 1]$ , which interpolates between two neighboring vacua when  $\tau$  changes from 0 to 1, there has to be at least one value  $\tau_0$  of  $\tau$  such that the Higgs field  $\phi(x, \tau_0)$  has a zero. In the case of the electroweak theory and the so-called minimal path which connects two neighboring vacua the sphaleron is precisely such a configuration. If we follow the minimal path we know that at the sphaleron there will be a normalizable eigenmode of the Dirac operator and it has zero eigenvalue. It is intuitively reasonable that a zero of the Higgs field is a necessary condition for having a zero eigenvalue of the full Dirac operator. However, there is to our knowledge no topological theorem which tells us that the full Dirac operator has eigenvalue zero for some  $\tau_0$ . This is in contrast to the case of the massless Dirac operator, which only couples to the gauge field, and where it follows from the Atiyah-Patodi-Singer index theorem that the number of eigenvalues of the Dirac Hamiltonian which crosses zero is directly related to the change in Chern-Simons number [7, 8, 9].

Recently a number of articles have addressed the question of level crossing for the full Dirac Hamiltonian in the electroweak theory [10, 11, 12]. The proof of the validity of the level crossing picture has either been of numerical nature, for a specific chosen path in  $(\phi, A_i)$  configuration space, or it has used some special symmetry properties of the sphaleron solutions and is only valid for some range of the coupling constants. In this article we make an attempt to investigate the validity of the level crossing picture in the case of fluctuations of the gauge *and especially the Higgs fields* which are typical for the high temperatures of the early universe.

There is one more reason to focus on the Higgs field. The role of this field in the high temperature fluctuations, and in particular its relation to the masses of the fermions and therefore to the level shifting, is not very clear. If the symmetry is restored the classical expectation value of the Higgs field is equal to zero, even if we have imposed complete gauge fixing. However, the field still couples to the fermions and the statement that  $\langle \varphi \rangle_T = 0$  refers to the thermal average  $\langle \cdot \rangle_T$ . When we discuss temperature induced transitions of gauge and Higgs fields between neighboring vacua connected by large gauge transformations we deal with dynamical processes caused by thermal fluctuations, and it is strictly speaking misleading to refer to thermal averages. In fact we want in the discussion of the anomaly and level shifting to use an approximation where the gauge and Higgs fields are treated as background fields *and even above the symmetry restoration temperature we can talk about “sphaleron-like” transitions*. In the simulations we perform the expectation value  $\langle |\varphi|^2 \rangle$  will typically be quite small compared to the classical vacuum expectation value  $\langle |\varphi|^2 \rangle_0$  at zero temperature, due to temperature fluctuations. This indicates that the system is in the symmetric phase rather than in the broken phase. It is nevertheless perfectly possible (for a finite volume) to talk about the fields as located in the neighborhood of a definite vacuum and the transition rate between such vacua. The picture becomes especially clear if one talks about the family of all fields which interpolate between the neighborhoods of two different vacua, and then focuses on those configurations in which the high energy thermal fluctuations have been stripped off. By such a procedure it becomes clear that the low frequency modes of the gauge fields can be viewed as interpolating between the different vacua and that the Chern-Simons number will change by one unit during the interpolation [3]. In this article we will use the spectral flow of the Dirac operator as a means to include the Higgs field in the analysis.

The rest of this article is organized as follows: In sec. 2 we define the “reduced” fermionic part of the electroweak model we will use. In sect. 3 we show how to discretize the corresponding Dirac Hamiltonian on a three-dimensional spatial lattice and especially how to define the concept of chirality on this lattice. Sec. 4 contains

the numerical analysis of level crossing and chirality change for a number of “hand made” families of gauge-Higgs configurations. This analysis is made to compensate for the lack of mathematically rigorous results for Dirac Hamiltonians coupled to chiral fermions, results which we need when interpreting the level shifting and chirality change in the numerical simulations. In sect. 5 we describe the numerical method used to simulate the gauge-Higgs part of the electroweak theory. Sect. 6 reports on the measurements of spectral flow of the Dirac operator for “sphaleron-like” transitions. Finally sect. 7 contains a discussion of the results obtained.

## 2 The model

Let us consider the electroweak theory where for simplicity we ignore the hypercharge sector. It is of no importance for the electroweak anomaly. We also restrict ourselves to two families. The generalization to the twelve existing doublets is trivial.

The fermionic part of the Lagrangian is given by:

$$\begin{aligned} \mathcal{L}_f = & \bar{\psi}_L \not{D} \psi_L + \bar{\chi}_R \not{\partial} \chi_R + \bar{\psi}'_L \not{D} \psi'_L + \bar{\chi}'_R \not{\partial} \chi'_R \\ & - \bar{\psi}_L (h_u \tilde{\varphi} \chi_{uR} + h_d \varphi \chi_{dR}) - (h_u \bar{\chi}_{uR} \tilde{\varphi}^\dagger + h_d \bar{\chi}_{dR} \varphi^\dagger) \psi_L \\ & - \bar{\psi}'_L (h'_u \tilde{\varphi} \chi'_{uR} + h'_d \varphi \chi'_{dR}) - (h'_u \bar{\chi}'_{uR} \tilde{\varphi}^\dagger + h'_d \bar{\chi}'_{dR} \varphi^\dagger) \psi'_L \end{aligned} \quad (3)$$

where the left handed doublets are

$$\psi_L = \begin{pmatrix} \psi_u \\ \psi_d \end{pmatrix}_L \quad \psi'_L = \begin{pmatrix} \psi'_u \\ \psi'_d \end{pmatrix}_L \quad (4)$$

and the four right handed singlets are  $\chi_{uR}, \chi_{dR}, \chi'_{uR}, \chi'_{dR}$ . With an abuse of notation we collect them as vectors, like the doublets, even if they of course behave like singlets under electroweak  $SU(2)$  transformations:

$$\chi_R = \begin{pmatrix} \chi_u \\ \chi_d \end{pmatrix}_R \quad \chi'_R = \begin{pmatrix} \chi'_u \\ \chi'_d \end{pmatrix}_R \quad (5)$$

The Higgs doublet  $\varphi$  and its conjugated field  $\tilde{\varphi}$  (which transforms as  $\varphi$  under electroweak transformations) are defined as usual:

$$\varphi = \begin{pmatrix} \phi_+ \\ \phi_0 \end{pmatrix}, \quad (6)$$

$$\tilde{\varphi} = \begin{pmatrix} \phi_0^* \\ -\phi_+^* \end{pmatrix} = i\tau_2 \varphi^* \quad (7)$$

There are four independent Yukawa couplings  $h_u, h_d, h'_u$  and  $h'_d$ . As mentioned above we have only two independent couplings in the corresponding lattice model

and for simplicity we therefore choose  $h'_u = h_u$  and  $h'_d = h_d$ .  $h_u \approx h_d$  mimics the quark sector (as the notation indicates), while  $h_d = 0$  describes the lepton sector.

It is well known that the chiral theory defined by (3) can be given a formulation as a vector-like theory of Dirac fermions [13]. This is due to the fact that the representations of  $SU(2)$  are real. We can therefore introduce the charge-conjugated fields

$$\psi'^c_R = \varepsilon C \psi'_L = \begin{pmatrix} \psi'^c_{dR} \\ -\psi'^c_{uR} \end{pmatrix} \quad (8)$$

where  $\varepsilon = i\tau_2$  acts on the isotopic indices and  $C$  is the charge-conjugation matrix, acting on spinor indices:  $\psi^c \equiv C\psi$ . In a similar way we define

$$\chi'^c_L = C \chi'_R = \begin{pmatrix} \chi'^c_{dL} \\ -\chi'^c_{uL} \end{pmatrix}. \quad (9)$$

If we use the chiral representation of the  $\gamma$  matrices a Dirac fermion can be written as

$$f_D = \begin{pmatrix} f_L \\ f_R \end{pmatrix}. \quad (10)$$

and we can now introduce the two Dirac spinors:

$$\psi_D = \begin{pmatrix} \psi_L \\ \psi'^c_R \end{pmatrix}, \quad \chi_D = \begin{pmatrix} \chi_R \\ \chi'^c_L \end{pmatrix}. \quad (11)$$

This allows us finally to introduce the *eight*-component spinor  $\Psi$  by:

$$\Psi = \begin{pmatrix} \psi_D \\ \chi_D \end{pmatrix}, \quad (12)$$

and using the matrix

$$M = \Phi \begin{pmatrix} h_u & 0 \\ 0 & h_d \end{pmatrix}, \quad \Phi = \begin{pmatrix} \phi_0^* & \phi_+ \\ -\phi_+^* & \phi_0 \end{pmatrix}, \quad (13)$$

we can write the Lagrangian (3) as follows

$$-\mathcal{L}_f = \bar{\Psi} \begin{pmatrix} \not{D} & -M \\ -M^\dagger & \not{\partial} \end{pmatrix} \Psi \quad (14)$$

such that each entry of the matrix in eq. (14) is a  $2 \times 2$  matrix in isospinor indices and a  $4 \times 4$  matrix in spinor indices.

Note that (14) resembles the ordinary Dirac equation but that (i) the mass is spatially varying, depending on  $\varphi$ , (ii) the mass term may multiply the 1st and 2nd (and 3rd and fourth) components differently if  $h_u \neq h_d$  and, most importantly, (iii) only the first 4 components ( $\psi_D$ ) of the eight component spinor  $\Psi$  have gauge interactions. The last four ( $\chi_D$ ) are gauge singlets.

The notation introduced here follows [11], which also introduced the generalized chirality matrix  $\tilde{\Gamma}_5$  acting on the eight component fermion field  $\Psi$ :

$$\tilde{\Gamma}_5 = \begin{pmatrix} \gamma_5 & 0 \\ 0 & -\gamma_5 \end{pmatrix}. \quad (15)$$

The matrix  $\tilde{\Gamma}_5$  anticommutes with the matrix in (14) and also with the matrix

$$\Gamma_0 = \begin{pmatrix} \gamma_0 & 0 \\ 0 & \gamma_0 \end{pmatrix} \quad (16)$$

which enters in the definition of  $\bar{\Psi}$ . Consequently the Lagrangian (14) is invariant under the generalized chiral transformation [11]

$$\Psi \rightarrow e^{i\theta\tilde{\Gamma}_5/2}\Psi, \quad \bar{\Psi} = e^{i\theta\tilde{\Gamma}_5/2}\bar{\Psi}. \quad (17)$$

The symmetry expresses nothing but the fermion number conservation of the electroweak theory. In fact the current associated with the symmetry is:

$$J_\mu^5 = \bar{\Psi}\gamma_\mu\tilde{\Gamma}_5\Psi = \bar{\psi}_D\gamma_\mu\gamma_5\psi_D - \bar{\chi}_D\gamma_\mu\gamma_5\chi_D, \quad (18)$$

or, expressed in terms of the original fields of the model:

$$J_\mu^5 = \bar{\psi}_L\gamma_\mu\psi_L + \bar{\psi}'_L\gamma_\mu\psi'_L + \bar{\chi}_R\gamma_\mu\chi_R + \bar{\chi}'_R\gamma_\mu\chi'_R \quad (19)$$

i.e. the fermionic current. As remarked in the introduction this current is known to be anomalous:

$$\partial_\mu J_\mu^5 = \frac{g_w^2}{32\pi^2} F_{\mu\nu}^a \tilde{F}^{a\mu\nu} \quad (20)$$

and leads to the famous non-conservation of baryon number in the electroweak theory. The reason we introduce the generalized chirality dictated by  $\tilde{\Gamma}_5$  is that the analogy to ordinary abelian symmetry and the level shifting picture will be more clear, as emphasized recently by several authors [11, 12], who proved that under certain assumptions a transition from one vacuum to another, related by a large gauge transformation, will result in a level shift. It is our goal to try to verify this level shifting for realistic high temperature configurations which do not necessarily satisfy the assumptions used in the analytical proofs of the level shifting and, in addition, to provide further evidence that we really observe continuum-like configurations during the simulations.

### 3 Lattice Formulation

First consider the time-independent continuum Dirac equation in a background temporal gauge-fixed field  $A_i = A_i^a \tau^a$ :

$$(i\alpha_i\partial_i + A_i\alpha_i + \beta m)\psi(x) = E\psi(x). \quad (21)$$

Here the index  $i$  runs over the three spatial directions, the wavefunction  $\psi$  is a gauge doublet (weak isospinor) with four spinor components acted on by the  $4 \times 4$  hermitian Dirac matrices  $\alpha_i$  and  $\beta$ . These satisfy

$$\{\alpha_i, \alpha_j\} = 2\delta_{ij} ; \{\alpha_i, \beta\} = 0 ; \beta^2 = 1. \quad (22)$$

For the purposes of this section it is again useful to consider the chiral representation of the  $\gamma$ -matrices, which means that the  $\alpha_i$  and  $\beta$  matrices are represented by:

$$\alpha_i = \begin{pmatrix} \sigma_i & \\ & -\sigma_i \end{pmatrix} ; \beta = \begin{pmatrix} & 1_{2 \times 2} \\ 1_{2 \times 2} & \end{pmatrix}, \quad (23)$$

where  $\sigma_i$  are the Pauli matrices.

On the lattice we will be using the staggered formulation for fermion fields.

### 3.1 The massless case

Let us in this section consider the massless limit  $m = 0$ . The lattice transcription of (21) reads

$$\frac{i}{2} \sum_{i=1}^3 \eta_i(x) [U_i(x) \chi(x + \hat{i}) - U_i^\dagger(x - \hat{i}) \chi(x - \hat{i})] = E \chi(x), \quad (24)$$

where  $\chi(x)$  is a *single* spin component isospinor field, the  $U_i$  are SU(2) valued link variables defined on the lattice links, which may be parameterized as  $\exp(iaA_i(x))$ , where  $a$  is the lattice spacing, and the  $\eta_i(x)$  are the Kawamoto-Smit phases defined as  $\eta_i(x) = (-1)^{x_1 + \dots + x_{i-1}}$ . It is well known that in the limit where the gauge field varies smoothly on the scale of the lattice spacing, the continuum limit of (24) recovers two copies of (21), which we interpret as describing two independent fermion species [15, 16]. These species become coupled by terms of higher order in  $a$  [17] (i.e. by momentum modes from the outer half of the Brillouin zone [18]).

For an arbitrary background link field there are important symmetries in the spectrum. If we denote by  $(\chi, E)$  the existence of an eigenmode  $\chi(x)$  with eigenvalue  $E$ , then

$$(\chi, E) \Leftrightarrow ((-1)^{x_1 + x_2 + x_3} \chi, -E), \quad (25)$$

and

$$(\chi, E) \Leftrightarrow (\tau_2 \chi^*, -E), \quad (26)$$

where the Pauli matrix  $\tau_2$  acts in weak isospace. Clearly applying both symmetries (25) and (26) implies that each mode is doubly degenerate. Compare with the symmetries of the continuum equation (21):

$$(\psi, E) \Leftrightarrow (\gamma_5 \psi, E), \quad (27)$$



where  $\gamma_5 \equiv i\alpha_1\alpha_2\alpha_3$ , and

$$(\psi, E) \Leftrightarrow (C\tau_2\psi^*, E), \quad (28)$$

where  $C \equiv i\alpha_1\alpha_3$  in the particular Dirac matrix representation (23). There is a third symmetry, which has no analogue for the lattice equation (24):

$$(\psi, E) \Leftrightarrow (\beta\alpha_1\alpha_2\alpha_3\psi, -E). \quad (29)$$

Symmetry (27) holds only for  $m = 0$ , whereas (28) and (29) hold for any  $m$ .

The matrix  $\gamma_5$  defines the chirality operator in the continuum formulation. In order to represent chirality in the lattice system, it is necessary to project onto the flavor singlet sector of the multiple-species algebra implicit in (24); ie. we need to define an operator  $\Gamma_5 = \gamma_5 \otimes 1_2$ , where the second matrix operates on a “flavor space” [17, 18]. For the four-dimensional Euclidean Dirac operator, this projection has been implemented by Smit and Vink in their programme to compute topological charge [19], and by Hands and Teper in studies of chiral symmetry breaking [20]. The basic algebraic steps are given in [17, 18]. For our three dimensional problem the algebra is very similar, and here we give simply the result:

$$\langle \chi_n | \Gamma_5 | \chi_n \rangle = \frac{i}{2^3} \sum_x \sum_{ijk=\pm 1} (-1)^{x_2} \chi_n^\dagger(x) \mathcal{U}_{111} \chi_n(x + i\hat{1} + j\hat{2} + k\hat{3}). \quad (30)$$

Here  $\chi_n(x)$  is the  $n$ th eigenmode, and  $\mathcal{U}_{111}$  denotes the average of the SU(2) link products over the six equivalent paths joining the two sites, thus ensuring the expectation value is gauge invariant. Notice there is an important difference with the continuum operator. Since  $\Gamma_5$  is a three-link operator,  $\Gamma_5^2 \neq 1$ ; only in the deep continuum limit will  $\Gamma_5$  and  $\gamma_5$  coincide. At non-zero lattice spacing  $\Gamma_5$  requires in principle a finite multiplicative renormalization, which may be estimated perturbatively [21] or numerically [19].

Now consider what happens at a level crossing, when an eigenmode crosses zero. There are never any exact zero modes in a lattice simulation, so we will refer to modes which approach zero as “quasi-zero modes”. Using the symmetries (25), (26) and the definition (30), we can see that if there is such a mode with energy  $\varepsilon$  and chirality  $\gamma$ , then there will also be a mode with energy  $-\varepsilon$  and chirality  $-\gamma$ . As we shall see in subsequent sections, a lattice level crossing has the following signal – a mode initially has energy  $\varepsilon$  and chirality  $\gamma_a$ ; as the simulation proceeds  $\varepsilon$  becomes smaller, eventually reaching a minimum before increasing again. The chirality  $\gamma$  should *reverse* sign at this point, eventually reaching a value  $-\gamma_b$ . Since each lattice mode is doubly degenerate, we interpret this process as *two* positive energy modes of chirality  $+\gamma_a$  crossing zero to become negative energy modes of chirality  $+\gamma_b$ , and, using symmetries (25), (26), *two* negative energy modes of chirality  $-\gamma_a$  crossing

zero to become positive energy modes with chirality  $-\gamma_b$ . The total change in chiral charge is thus  $\Delta Q = -2(\gamma_a + \gamma_b)$ . In the continuum limit as  $\Gamma_5$  approximates  $\gamma_5$  we should find  $|\gamma|$  approaching 1. Thus we find  $|\Delta Q| \simeq 4$ , which should be compared with the result for level crossing for the continuum Dirac Hamiltonian of  $|\Delta Q| = 2$ : the extra factor of two is a consequence of species doubling for lattice fermions. We shall see in the following sections how well these ideal criteria are met in actual lattice simulations.

### 3.2 Masses and Yukawa coupling

The situation becomes more complicated once a fermion mass is introduced. As argued in [22], the algebra (22) obeyed by  $\alpha_i$  and  $\beta$  is identical to that of the hermitian Euclidean matrices  $\gamma_\mu$  in a covariant formulation, which requires a four-dimensional lattice in order to be represented faithfully by staggered fermions. Therefore to incorporate mass we introduce a second ‘‘timeslice’’ of link variables, identical to the first, and couple it to the original one as if it were displaced by one unit in a fictitious Euclidean time direction. The lattice equation becomes

$$\frac{i}{2} \sum_i \eta_i(x) [U_i(x) \chi(x + \hat{i}) - U_i^\dagger(x - \hat{i}) \chi(x - \hat{i})] + m \eta_4(x) \chi(x + \hat{4}) = E \chi(x), \quad (31)$$

ie. as if it were formulated on a  $N^3 \times 2$  lattice with periodic boundary conditions assumed in the 4th direction. The phase factor  $\eta_4(x) = (-1)^{x_1+x_2+x_3}$ . Whether we regard this extra degree of freedom as an extra timeslice connected to the first by unit gauge connections, or simply as an extra component of the wavefunction  $\chi$  is a matter of taste: the result is that we have a system which in the continuum limit now describes four species of four-component fermions. There are the following symmetries in the spectrum:

$$(\chi, E) \Leftrightarrow ((-1)^{x_1+x_2+x_3+x_4} \chi, -E); \quad (32)$$

$$(\chi, E) \Leftrightarrow (\tau_2 (-1)^{x_4} \chi^*, -E). \quad (33)$$

As before, these symmetries ensure that each lattice mode is two-fold degenerate. However, the fact that the modes with energy  $-E$  have minus the chirality of the mode with energy  $E$  remains unaltered. It is also important to note that the chirality operator (30) links lattice sites in the *same* timeslice: therefore chirality for eigenmodes of the massive equation (31) is simply the sum of chiralities for each of the timeslices considered individually:

$$\langle \chi_n | \Gamma_5 | \chi_n \rangle = \langle \chi_{1n} | \Gamma_5 | \chi_{1n} \rangle + \langle \chi_{2n} | \Gamma_5 | \chi_{2n} \rangle. \quad (34)$$

In this equation  $\chi_{1n}(x)$  is an eigenvector of (31) projected onto the first timeslice, and  $\chi_{2n}(x)$  the same eigenvector projected onto the second timeslice. We shall see that once mass is introduced, the minimum value of  $|E|$  is  $m$ , and that the chirality as measured by (30) tends to have opposite signs on each of the two timeslices, thus reducing the overall expectation. This is in accordance with our continuum intuition that a mass term couples fields of opposite chirality.

Finally we discuss the incorporation of Yukawa interactions with a Higgs field, so that the standard model can be discussed. Once again we begin with the continuum formulation: if we use the explicit representation of the Dirac matrices (23) we may according to the Lagrangian (14) write the equations of motion (suppressing the primed fields, which are not essential to the formulation) as

$$\begin{pmatrix} i\sigma_i D_i & M \\ M^\dagger & -i\sigma_i \partial_i \end{pmatrix} \begin{pmatrix} \psi_L \\ \chi_R \end{pmatrix} = E \begin{pmatrix} \psi_L \\ \chi_R \end{pmatrix}, \quad (35)$$

where each entry is a  $2 \times 2$  matrix in spinor space and a  $2 \times 2$  matrix in isospace. The resulting system is very similar to the Dirac equation for *four*-component Dirac spinors (recall the comments following (14)). Now, to model a mass term in the original system, i.e. to incorporate a prescription for the matrix  $\beta$ , recall that we doubled the number of spinor components by introducing a second timeslice with identical gauge interactions, and had the mass terms couple the two slices. Here we will do the same, except that on the second timeslice, corresponding to the  $\chi$  components, there will be no gauge interactions. Gauge invariance will be enforced as in the continuum by coupling the Higgs fields to the  $\psi$  fields on the original timeslice. The system of lattice equations then reads

$$\frac{i}{2} \sum_i \eta_i(x) [U_i(x) \psi(x + \hat{i}) - U_i^\dagger(x - \hat{i}) \psi(x - \hat{i})] + \eta_4(x) M(x) \chi(x) = E \psi(x), \quad (36)$$

$$\frac{i}{2} \sum_i \eta_i(x) [\chi(x + \hat{i}) - \chi(x - \hat{i})] + \eta_4(x) M^\dagger(x) \psi(x) = E \chi(x), \quad (37)$$

where  $\psi$  and  $\chi$  are now single spin-component gauge-doublet fields. The following symmetries exist:

$$(\psi, \chi, E) \Leftrightarrow (\eta_4 \psi, -\eta_4 \chi, -E), \quad (38)$$

and, if  $h_u = h_d$ ,

$$(\psi, \chi, E) \Leftrightarrow (\tau_2 \psi^*, -\tau_2 \chi^*, -E). \quad (39)$$

Once again, these symmetries ensure that each lattice mode is doubly degenerate if  $h_u = h_d$ ; if not, there will be an additional fine structure in the spectrum.

Because of the symmetry of the spectrum about  $E = 0$ , the system described by the lattice Hamiltonian (36)-(37) is not truly chiral: if it were there would be spectral asymmetry, and true spectral flow would result when a mode crossed zero.

Of course, the reason the model is not chiral is due to the species replication inherent to the lattice approach (we leave aside the issue of the requirement for complex representations, since in any case it is perfectly possible to introduce a  $U(1)_Y$  gauge interaction in the lattice system). For every positive energy level which crosses zero to become negative, there will be a corresponding negative energy level crossing zero to become positive. The symmetries (38),(39) ensure that at each zero crossing *four*  $SU(2)$  doublets are involved: two cross one way and two the other. Thus there is no true baryogenesis on the lattice, since for each unit of baryon number created there is another one destroyed. Of course, in the continuum limit we expect the species to become independent (in the quenched approximation), and thus we should be able to focus simply on the crossing itself as the event of interest. Note also that chirality is still defined by (30), and that we have the freedom to either define the total chirality of the mode as  $\langle\psi|\Gamma_5|\psi\rangle + \langle\chi|\Gamma_5|\chi\rangle$ , or the more sophisticated version  $\langle\psi|\Gamma_5|\psi\rangle - \langle\chi|\Gamma_5|\chi\rangle$ . As we saw in sect. 2 it is the last version which is directly related to the anomalous fermion number of the electroweak theory and we will use this definition in the following:

$$\langle\Psi|\tilde{\Gamma}_5|\Psi\rangle \equiv \langle\psi|\Gamma_5|\psi\rangle - \langle\chi|\Gamma_5|\chi\rangle, \quad \Psi \equiv \begin{pmatrix} \psi \\ \chi \end{pmatrix} \quad (40)$$

## 4 Calibration

As mentioned above there seem not to be any analytical results which tell us in detail about the level crossing for chiral fermions coupled to the gauge-Higgs system encountered in the standard model. In order to know what to expect we have investigated this question numerically on the lattice by taking families of smooth configurations<sup>4</sup> which interpolate between different classical vacua and for these configurations we have followed the flow of eigenvalues and the change of chiralities. We have investigated the following scenarios:

- (1) A family of gauge-Higgs field configurations which interpolate between two vacua and where the zero of the Higgs field appears at the same time as the Chern-Simons number  $N_{cs}(t)$  of the gauge field is equal to  $1/2$ .
- (2) A family of field configurations where the gauge- and Higgs fields still interpolate between two vacua, but where the zero of the Higgs field is displaced in time relative to the time  $t$  where  $N_{cs} = 1/2$ .

---

<sup>4</sup>By “smooth” configurations we mean lattice configurations which are approximations to continuum configurations.

- (3) A family of field configurations where only the gauge field interpolates between two neighboring gauge vacua, while the Higgs field remains constant.
- (4) A family of field configurations where only the Higgs field interpolates between two neighboring Higgs vacua, while the gauge field stays constant (for instance zero).

The field configurations are constructed as follows: Let us first define a gauge transformation  $V(x)$  with winding number one:

$$V(x) = (-1) \exp \left( \frac{2\pi i \sigma_i v_i}{L |v(x)|} \max\{|v_j(x)|, j = 1, 2, 3\} \right), \quad (41)$$

where  $x$  denotes a lattice point,  $L$  the linear size of the lattice,  $v_i = x_i - \frac{1}{2}L$  and  $\sigma_i$  are the Pauli matrices. The trivial vacuum is given by

$$U_i^{(0)}(x) = \hat{1}, \quad \phi^{(0)}(x) = \begin{pmatrix} 0 \\ 1 \end{pmatrix}, \quad (42)$$

while a vacuum configuration with winding number one is given by

$$U_i^{(1)}(x) = V(x)V^{-1}(x + \hat{e}_i) = \exp(i\sigma_i u_i(x)) \quad (43)$$

$$\phi^{(1)}(x) = V(x)\phi^{(0)}. \quad (44)$$

where  $\hat{e}_i$  is a unit lattice vector in direction  $i$  and  $u_i(x)$  will be close to zero for large lattices.

A continuous family of configurations which interpolate between the two vacua is simply given by

$$U_i(x, t) = \exp(if(t)\sigma_i u_i(x)), \quad (45)$$

$$\phi(x, t) = (1 - g(t))\phi^{(0)} + f(t)\phi^{(1)}(x), \quad (46)$$

where  $f(t)$  and  $g(t)$  are monotonic, continuous functions which interpolate between 0 and 1 when  $t$  changes from 0 to the final time which we denote  $T$ .

Note that there exists precisely one space-time point  $(x, t)$  where  $\phi(x, t) = 0$  and the time  $t$  is determined by  $1 - g(t) = f(t)$ . We denote this time  $t_h$ . If  $g(t) = f(t)$  it will coincide with the time  $t_{1/2}$  where  $N_{cs}(t) = 1/2$ , but if  $g \neq f$  it will in general be different from  $t_{1/2}$ .

We will choose  $f(t) = t/T$  in the actual numerical calculations. This means that  $t_{1/2} = T/2$ . In case (1) and (4) mentioned above we choose  $g(t) = f(t)$ . In case (2) we choose  $g(t) = \min\{3t/T, 1\}$ , which means that the zero of the Higgs field will be located at  $t = T/4$ , ( $t_h = T/4$ ) i.e. displaced by  $T/4$  relative to  $t_{1/2}$ .

Let us now describe the spectral flow and the change in chirality for the four families of field configurations mentioned above. In fig. 1 we show the Chern-Simons number as a function of the time  $t$  for the gauge fields given by (45). In addition we show in fig. 2 the change in the lowest eigenvalue and the change in chirality for various values of the Yukawa coupling. Everything behaves as expected from the continuum considerations.

In case (2) where the zero of the Higgs field is displaced from  $t_{1/2}$  we see that the time  $t_0$  at which the lowest eigenvalue crosses zero changes continuously with increasing Yukawa coupling from  $t_{1/2}$ , corresponding to the crossing at  $N_{cs} = 1/2$  for zero Yukawa coupling, towards  $t_h$ , which is the time where the Higgs field has a zero. This is illustrated in fig. 3. The flip in chirality always occurs at  $t_0$ , as expected.

In case (3) where the Higgs field is constant we see that the level crossing is still present for moderate values of the Yukawa coupling. This is in sharp contrast to the situation where we insert an explicit mass term in the Dirac equation. In that case we know from the continuum equation that there is a mass gap, separating the negative and the positive eigenvalues, and this is also seen explicitly in the lattice implementation (see sec. 6). When the Yukawa coupling is increased  $t_0$  is gradually displaced towards  $T$ , and for a finite value of the Yukawa coupling  $t_0$  reaches  $T$  and there is no longer any level crossing and no chirality flip. This scenario is shown in fig. 4.

The behavior of the lowest eigenvalue in the situation where the gauge field is zero (i.e.  $U_i(x)$  is given by (42)) and Higgs field is given by (46) with  $g(t) = f(t) = t/T$  is shown in fig. 5 as a function of the Yukawa coupling. The situation is in a certain sense dual to the one in case (3). For small Yukawa coupling there is no level crossing, but eventually a zero and a corresponding chirality flip takes place at  $T$  and with increasing Yukawa coupling  $t_0$  moves towards  $t_h$ .

The results in this section are relevant when we want to interpret the data obtained in real lattice simulations. In particular we see that increasing the Yukawa coupling can displace the time  $t_0$  of zero level crossing. It is somewhat surprising that there is no need for a zero in the Higgs field in order to observe level crossing, provided the Yukawa coupling is sufficiently small. However, our three dimensional lattice has periodic boundary conditions and since it is finite, it imitates a compact space of finite volume. This means that the ‘‘continuum’’ configuration imitated by (45) for the gauge field and (42) for the Higgs field will have finite energy, and we expect spectral flow of the continuum Dirac operator to be continuous with respect

to the coupling constants in the lagrangian. Since we have level crossing for zero Yukawa coupling by the Atiah-Singer index theorem and since the chiral symmetry is not broken for finite Yukawa coupling, we must have level crossing for small Yukawa couplings as well, even if the Higgs field is nowhere zero. This is indeed what we observe. For sufficiently large Yukawa coupling the level crossing can disappear without violating any continuity requirements by the mechanism shown in fig. 4. It is more difficult to decide whether these continuity arguments remain valid if the three dimensional space is non-compact. The very simple configurations we have used will have infinite energy in the non-compact case and might not belong to a reasonable class of field configurations where one can define a spectral flow of the Dirac operator  $H(A_i(t), \phi(t))$ . Similar remarks are valid in case (4). On the other hand the results obtained in case (2) are probably true also for a non-compact continuum space, even if the actual configuration used here has infinite energy in the continuum limit for  $t \neq 0, T$ . The reason is that it is easy to find finite energy continuum field configurations with the characteristics used in case (2). An analytic proof of the behavior observed in case (2) has recently been given if space is one dimensional [26]. It would be interesting to extend it to three dimensions.

At high temperature we might certainly encounter situations where the phase of the Higgs and the gauge field are placed in different gauge sectors as in case (3) or (4), since the finite temperature provides the needed infinite energy. Consequently cases (3) and (4) are relevant for our interpretation of data not only because the spatial lattice used in the simulations is finite, but also because the situations might be generic at the high temperatures prevailing in the early universe above the electroweak phase transition.

## 5 The numerical method

### 5.1 The approximation

The following approximations have been used in this work: we consider only one weak isospinor fermion and the two associated singlet fermions and we ignore the hypercharge sector. These approximations are presumably not important for the questions we want to address. In addition we completely ignore the feedback of fermions on the gauge and Higgs fields and we always treat the gauge and Higgs fields as background fields when we ask dynamical questions about the fermions. This approximation is difficult to control, but it might still not be very important for the dynamics of the gauge and Higgs fields. The basic approximation, when it comes to the dynamics of the gauge and Higgs fields, is the use of classical physics

as the tool for simulating the high temperature fluctuations in the electroweak theory. One would expect this approximation to give a reliable representation of the magnetic sector of the theory since the classical partition function on the lattice<sup>5</sup> is identical to the naive infinite temperature limit of the full quantum partition function. If we discuss the electric properties of the theory it is by now well known that we need to supplement the naive dimensional reduction with mass and charge renormalizations and in addition with Higgs fields in the adjoint representation (the remnants of the  $A_0$  component) in order to get a correct representation of the full quantum theory [14]. The Gauss constraint will be satisfied by the use of the classical equations, and this means that the kinetic part of the adjoint Higgs field coupled to the gauge field *will* be included in the classical approximation (The Gauss constraint is equivalent to a term  $(D_i^\dagger A_0)^a (D_i A_0)^a$  in the Lagrangian). However, there will be additional terms like  $A_0^2$ ,  $A_0^4$  and  $A_0^6$  in the effective three-dimensional high temperature expansion of the action, where especially the first two terms are important for the Debye screening mass. We will ignore these subtleties here<sup>6</sup> and view the present computer simulations as generating typical high temperature fluctuations, the temperature being judged to correspond to fluctuations in the unbroken phase since  $\langle \varphi^2 \rangle$  is significantly smaller than its tree value for the choice of lattice coupling constants we will use (see later).

Classical thermal fluctuations can be generated either by using a canonical ensemble and applying some standard Monte Carlo updating like heat bath or the Metropolis algorithm to the field configuration, or (more fundamentally) to use a micro-canonical ensemble and just let it develop according to the classical equations of motion. In the first case the temperature is kept fixed, while the energy per degree of freedom will have fluctuations proportional to  $1/\sqrt{N}$ ,  $N$  being the number of degrees of freedom. In the second case the energy will be constant, while the temperature of the system will fluctuate as  $1/\sqrt{N}$ . From a numerical point of view the first method is preferable, since the second is known to suffer from problems with ergodicity for too small systems. We have nevertheless chosen to use the classical equations of motion since they reflect very directly the real time evolution of the field configurations. However, in order to use the classical equations of motion we have to prepare an initial distribution of fields and their conjugate momenta corresponding

---

<sup>5</sup>Let us remind the reader that there exists no classical partition function of a continuum field theory due to the Rayleigh-Jeans instability. If one restricts the number of degrees of freedom per unit volume by considering a lattice version of the field theory the concept of a classical partition function is perfectly well defined.

<sup>6</sup>The role of these additional finite temperature corrections is not clear for the kind of questions we will deal with. Leaving aside the question of a gauge invariant meaning of the Debye screening mass, it is a static quantity, calculated as a temperature average in a canonical ensemble, while we consider dynamical processes such as sphaleron transitions which occur in real time.



to a given temperature, and here we have to use the heat bath or the Metropolis algorithm. For systems with gauge invariance this means additional complications since the Gauss constraint has to be satisfied for the classical configurations and this will not be the case for a Metropolis updating. This technical obstacle can be circumvented by introducing the Gauss constraint as a Lagrange multiplier (we refer to [2] for details). After the initial thermalization by means of Metropolis, we let the system develop according to the classical equations, discretized in a way which automatically conserves the Gauss constraint (see next subsection). For sufficiently large systems the fundamental hypothesis of ergodicity of the micro-canonical ensemble will ensure that the phase space surface of constant energy is covered uniformly if the system evolves according to the classical equations of motion.

## 5.2 The gauge-Higgs system

As mentioned above the sequence of gauge and Higgs field configurations we are using is generated by the classical equations of motion. By that we mean the following: we choose the standard Wilson action for Euclidean lattice gauge theory combined with the standard Higgs action on a lattice and make the obvious change of sign of the spatial part relative to the temporal part in order to get a Minkowskian signature. After that we make the lattice spacing in the temporal direction much smaller than in the spatial directions by scaling the lattice spacing “ $a$ ” to “ $a\Delta t$ ”. In this way the action will be split into a kinetic and a potential part:

$$S = \sum_t (E_{kin} - E_{pot}) \quad (47)$$

where the summation is over all time slices. From  $S$  one can derive the classical equations of motion which connect timeslice  $t$  and  $t + \Delta t$ . These equations of motion will automatically satisfy the Gauss constraint.

If we define an energy functional  $H$  by

$$H = E_{kin} + E_{pot} \quad (48)$$

it will not be strictly conserved by the equations of motion since time is still discrete. However, in the limit  $\Delta t \rightarrow 0$ ,  $H$  reduces to the correct Hamiltonian of the system and the energy will be conserved by the equations of motion. For  $\Delta t \leq 0.05$  we have, for the range of coupling constants used in the simulations, found very good conservation of the energy.

For a detailed discussion of the equation of motion derived from (47) we refer to [2]; let us only here give explicitly the form of  $\sum_t E_{kin}$  and  $\sum_t E_{pot}$  used in the

simulations:

$$\begin{aligned} \sum_t E_{kin} &= \frac{\beta_G}{(\Delta t)^2} \sum_{\square(t)} \left(1 - \frac{1}{2} \text{Tr} U_{\square(t)}\right) + \\ &\quad \frac{\beta_H}{2(\Delta t)^2} \sum_{x,t} \text{Tr} \left( \Phi_x^\dagger \Phi_x - \Phi_x^\dagger U_{x,x+\hat{0}} \Phi_{x+\hat{0}} \right) \end{aligned} \quad (49)$$

$$\begin{aligned} \sum_t E_{pot} &= \beta_G \sum_{\square(s)} \left(1 - \frac{1}{2} \text{Tr} U_{\square(s)}\right) + \frac{\beta_H}{2} \sum_{x,t,i} \text{Tr} \left( \Phi_x^\dagger \Phi_x - \Phi_x^\dagger U_{x,x+\hat{i}} \Phi_{x+\hat{i}} \right) \\ &\quad + \beta_R \sum_{x,t} \left( \frac{1}{2} \text{Tr} \Phi_{x,t}^\dagger \Phi_{x,t} - v^2 \right)^2 \end{aligned} \quad (50)$$

where  $U_{x,x+\mu}$  is the lattice gauge field on the link connecting  $x$  and  $x+\mu$ ,  $U_{\square}$  denotes the plaquette action for the gauge field and  $\square(t)$  stands for a plaquette in the  $\hat{0} - \hat{i}$  plane while  $\square(s)$  refers to a plaquette in a  $\hat{i} - \hat{j}$  plane. The  $SU(2)$  Higgs doublet  $\varphi$  is represented as a matrix

$$\Phi \equiv \begin{pmatrix} \phi_0^* & \phi_+ \\ -\phi_+^* & \phi_0 \end{pmatrix}. \quad (51)$$

The summation over spatial points is finite and limited by the lattice 3-volume (periodic boundary conditions) while it is infinite in the time direction.

The Metropolis updating used to thermalize the system uses as weight

$$\exp(-H_\xi), \quad H_\xi = H + \xi G^2 \quad (52)$$

where  $H$  is the lattice hamiltonian given by (48), while  $G$  denotes the lattice version of Gauss constraint (see [2] for details). By choosing  $\xi$  sufficiently large one can (at the expense of slowing down the thermalization time) control the violation of Gauss constraint to be arbitrarily small in the Metropolis updating.

If we write the classical continuum Hamiltonian as

$$H = \int d^3x \left[ \frac{1}{2} E_i^a E_i^a + \frac{1}{4} F_{ij}^a F_{ij}^a + |\pi|^2 + |D_i \varphi|^2 + \lambda(|\varphi|^2 - v_c^2)^2 \right] \quad (53)$$

the tree value connection between the lattice parameters in (49), (50) and the continuum coupling constants in (53) is as follows<sup>7</sup>

$$M_c^2 = \frac{2(1 - 2\beta_R - 3\beta_H)}{\beta_H a^2}, \quad \lambda_c = \frac{8\beta_R}{\beta_H^2}, \quad g_c^2 = \frac{4}{\beta_G} \quad (54)$$

where  $a$  denotes the lattice spacing and

$$v_c^2 a^2 = \frac{\beta_H}{2} v^2 = \frac{\beta_H}{4\beta_R} (2\beta_R + 3\beta_H - 1). \quad (55)$$

---

<sup>7</sup>We keep this unnecessary complicated notation for historical reasons

The naive continuum limit  $a \rightarrow 0$  imposes a fine tuning on  $(2\beta_R + 3\beta_H)$ . If we ignore thermal fluctuations and determine the  $W$ -mass  $M_W$  and the Higgs mass  $M_H$  from the coupling constants in the Hamiltonian we have:

$$M_H^2 a^2 = \frac{16\beta_R}{\beta_H} v^2, \quad M_W^2 a^2 = \frac{\beta_H}{\beta_G} v^2. \quad (56)$$

If for convenience, to restrict the coupling constant space, we impose the constraint  $M_W = M_H$ , we get the relation

$$\beta_R = \frac{\beta_H^2}{16\beta_G}. \quad (57)$$

From [2] we know that a reasonable choice is  $\beta_G \geq 10$  and  $\beta_H$  in the neighborhood of 1/3. This means that  $\beta_R$  is quite small.

### 5.3 The procedure

Equipped with an initial configuration at a given temperature and the classical equations of motion we can now follow the evolution of the Chern-Simons number by measuring the integral

$$Q(t) \equiv N_{CS}(t) - N_{CS}(0) = \frac{1}{32\pi^2} \int_0^t dt \int d^3x F_{\mu\nu}^a F^{a\mu\nu}. \quad (58)$$

This quantity has a simple implementation on the lattice and will directly give us the change in Chern-Simons number, which is a gauge invariant quantity. This procedure has been applied successfully before (see [2] for details). The typical measurement of  $Q(t)$  will result in a curve which stays for some time around integer values of  $Q(t)$ , while the transitions between these values take place rather rapidly. Superimposed on these movements of  $Q(t)$  will be short wavelength thermal fluctuations, which occasionally can mask somewhat the picture of  $Q(t)$  jumping between integer values. If desired, it is possible to strip off these thermal fluctuations in the following way. By solving the classical equations of motions we get a time sequence of configurations. For each of these configurations we can apply the simplest relaxation equation:

$$\frac{\partial\varphi}{\partial t} = -\frac{\delta H}{\delta\varphi}, \quad \frac{\partial A}{\partial t} = -\frac{\delta H}{\delta A} \quad (59)$$

where  $H$  is the Hamiltonian (48). This technique is well known from the lattice study of monopoles and instantons [20, 22, 23, 24, 25]. If one ‘‘cools’’ the configurations too much one forces them to a vacuum configuration, which is not what we want. However, only a few cooling steps will reduce the energy of the gauge configurations by a factor 80 without breaking the link to the original configuration since the

part of the field configurations which survives this relaxation is precisely the long wavelength fluctuations which we imagine are responsible for the large scale changes of  $Q(t)$ . Indeed, the picture of the transitions between different integer values of  $Q(t)$  is considerably sharpened by such a cooling. This effect is illustrated in fig. 6.

In order to check for level crossing during the time-development of the gauge field configurations we calculate the eigenvalues of the Dirac Hamiltonian for each time step, using the staggered fermion formalism discussed in detail in sections 2 and 3. Since the Dirac operator  $H_D(A(t), \varphi(t))$  will depend implicitly on the time  $t$  due to the time dependence of the gauge and Higgs field we will get a spectral flow of the eigenvalues and we can compare this with the expectation that a crossing of zero should be related to a change in Chern-Simons number and that diving and rising eigenvalues have different generalized chiralities.

The spectrum of the Dirac operator was found numerically by first using the Lanczos algorithm to tridiagonalize the hermitian Hamiltonian matrix, and then using Sturm bisection to extract the eigenvalues. As described in [20], on large systems this procedure finds eigenvalues iteratively, with convergence tending to occur first for extremal values of  $|E|$ . We found that for the systems we investigated the smallest eigenvalue converged after roughly 300 iterations of the Lanczos algorithm, and the lowest ten eigenvalues after roughly 700 iterations. Once the eigenvalues had converged the eigenmodes of the tridiagonal matrix are easily extracted by inverse iteration: the Lanczos algorithm is then rerun with the same initial vector in order to perform a unitary transformation on the eigenvectors of the tridiagonal matrix to convert them to eigenvectors of the original Hamiltonian. We checked that the resulting residual vectors had norms in the range  $10^{-6} - 10^{-10}$ , which is adequate for the subsequent measurements of chirality.

## 6 The measurements

### 6.1 Results for the massless Dirac operator

In [3] the spectral flow of the *massless* Dirac operator<sup>8</sup> was investigated along the lines outlined above. It was shown that there indeed was a crossing of zero associated with a sphaleron-like transition where the Chern-Simons number changed by one unit. Some questions were left unanswered, however.

The first question was connected with the chirality. As explained in sect. 3 the spectrum is symmetric with respect to energy  $E = 0$ . If an eigenvalue of chirality +1

---

<sup>8</sup>By “massless” we mean that the mass is explicitly chosen zero and that there is no coupling to the Higgs field.

crosses zero from above, a corresponding eigenvalue of chirality -1 should cross zero from below. This is indeed what we observe. In fig. 6 we have shown the change in Chern-Simons number which characterizes a typical sphaleron-like transition. In fig. 7 we show the corresponding diving of the lowest eigenvalue and the associated change in chirality.

The second question was related to the observation that a number of configuration histories had a Chern-Simons number which changed by  $1/2$  and then returned to its original value. These changes survived relaxation and they should consequently have some topological content. This hypothesis was supported by observing that their appearance was accompanied by a diving of eigenvalues to zero. It was conjectured in [3] that one could view such configurations as gauge-Higgs configurations which climbed to the sphaleron barrier where the Chern-Simons number is  $1/2$ , but then rolled back down to the original vacuum rather than to the neighboring one. By measuring the chirality we can substantiate these conjectures. This is illustrated in fig. 8, where we show such a situation. The eigenvalues vanish twice, the two zeroes being quite close, while the chirality at the first zero changes from  $+1$  to  $-1$  and back again to  $+1$  at the second zero. The obvious interpretation is that the field configurations reach a “sphaleron”-like configuration (where the energy is zero) and that it also overshoots it a little causing the negative chirality state to cross zero, but afterwards it returns to its original vacuum in agreement with a total change of Chern-Simons number of zero, and once again the chirality states cross zero.

We conclude that the gauge fields seem to qualify as continuum configurations. The change in Chern-Simons number is reflected closely in the spectral flow of the eigenvalues of the massless Dirac operator, which is implemented by means of staggered fermions.

## 6.2 Massive fermions

Before we turn to the “complete” electroweak theory, where the fermions acquire their masses via the Higgs field, it is illuminating to address the coupling of the gauge field to the massive fermions as discussed in sec. 3. In this case the continuum fermion is a four-component Dirac spinor and has isospin  $1/2$ . Recall that the lattice implementation uses two fields with support on alternating time slices to represent the lattice version of the Dirac matrix  $\beta$ , and chirality for a given eigenmode is defined by (34)<sup>9</sup>.

In this case the eigenvalues of the Dirac operator do not cross zero if solved in

---

<sup>9</sup>It makes no sense to use the generalized chirality  $\tilde{\Gamma}_5$  since the spinors in this case do not split into different isospin representations

a sequence of gauge field configurations where the Chern-Simons number changes by one. In fig. 9a we show the lowest eigenvalue for a number of different masses and we see that the lowest eigenvalue is approximately equal to the mass  $m$ , in agreement with expectations from the continuum formalism. We have studied the chirality of the lowest mode as a function of the mass. Some results are shown in fig. 9b. If the mass is zero the component  $\chi_{2n}(x)$  (see (34)) on the second timeslice does not contribute to the chirality as defined by (34). However even for small masses both components will start to contribute, but the sum for small masses is quite similar to that obtained in the massless case. However, as the mass increases  $\langle \Gamma_5 \rangle$  decreases towards zero, due to a cancellation between the contributions from the two timeslices. For the lowest eigenmode it seems still possible to observe a change in sign of  $\langle \Gamma_5 \rangle$  even for large masses. If we look at higher eigenmodes the chirality is closer to one and is less affected by the mass term. All this is in agreement with expectations from the continuum theory and verifies that the “two-timeslice” formalism works satisfactorily. We are now ready to apply the formalism to the electroweak theory.

### 6.3 Spectral flow of the full Dirac operator

In the following we will assume, unless explicitly mentioned, that  $h_u = h_d$  and we will denote the common coupling constant by  $h_y$ . We have investigated the level crossing picture and the change in the generalized chirality  $\tilde{\Gamma}_5$  for a number of sequences of configurations, each sequence corresponding to a change in Chern-Simons number of order one. For each of these sphaleron-like transitions the eigenvalues and eigenmodes of the Dirac equations (36),(37) were found for different values of the Yukawa coupling  $h_y$  ranging from 0.05 to 1. In addition these measurements were performed for three different “versions” of the same sphaleron-like transition, corresponding to different degrees of relaxation of the individual configurations, more precisely 0, 4 and 8 relaxation steps in the discretized version of eq. (59), which had the effect of stripping off as much as 96 % of the short wavelength thermal energy in the case of 8 relaxation steps.

The picture is very consistent for the various transitions and we will present details from two of them. In fig. 10a and 11a we have shown the lowest eigenvalue for the two sequences of configurations (parametrized by the time  $t$ ) near sphaleron transitions for Yukawa couplings  $h_y = 0.1, 0.25$  and  $0.5$  (fig. 10a) and  $h_y = 0.1$  and  $0.5$  (fig. 11a). In fig. 10b and 11b we have shown the measured generalized chirality  $\langle \tilde{\Gamma}_5 \rangle$  for the same sequences of configurations and the same values of the Yukawa coupling. 8 relaxation steps have been imposed on the configurations. The next to

lowest eigenvalues are only weakly affected and the same holds for the corresponding  $\langle \tilde{\Gamma}_5 \rangle$  values and we have chosen not to show these.

The effect of the relaxation is to increase the value of  $\langle \tilde{\Gamma}_5 \rangle$  slightly, and to affect only rather weakly the lowest eigenvalues in the case where  $h_y = 0.1$ . If  $h_y = 0.5$  the effect of cooling is somewhat stronger. This is shown in fig. 12 for the transition shown in fig. 11. In fig. 12a and 12b  $h_y = 0.1$  and three curves are shown of the lowest eigenvalue and  $\langle \tilde{\Gamma}_5 \rangle$ , respectively, corresponding to 0, 4 and 8 relaxation steps. The lowering of  $\langle \tilde{\Gamma}_5 \rangle$  in the case of no relaxation is in accordance with the discussion in sec. 3 and is presumably caused by fluctuations of the Higgs field. In fig. 12c and 12d we show the same set of curves, but generated for  $h_y = 0.5$ . It is clear from the figures that it will be difficult to conclude anything about level crossing and chirality flip of  $h_y > 0.5$  without relaxation of the individual configurations. When  $h_y \geq 1$  it is impossible even with extensive relaxation. For such large values of  $h_y$  there seems to have been introduced a lot of spurious transitions due to the fluctuations of the radial part of the Higgs field.

It is of interest to understand the relationship between the Higgs field and the transition between positive and negative chirality. As we increase the Yukawa coupling we indeed observed some change in the precise location of the “zero” energy solution<sup>10</sup> as is clear from fig. 10b and 11b. The change is small compared to the total width of the sphaleron-like transition (the region where the Chern-Simons number change by approximately one unit), but it nevertheless shows that there cannot be a strict relation between the zeros of the Higgs fields and the occurrence of a zero mode. This is in complete agreement with the analysis performed in section 4, where we used artificial “smooth” configurations. On the other hand we have to say that our setup is not the best for an investigation of such a relationship. The reason is that we are in the symmetric phase of the electroweak theory. The expectation value of the Higgs field is quite small and it fluctuates significantly. This means that  $\phi(x, t)$  might get close to zero in a number of places and the relaxation we use is insufficient to change the expectation value of the Higgs field very much. The phases of the Higgs and the gauge field seem to align much faster. This is due to the small value of the Higgs coupling which is dictated by the formal continuum limit. It would be interesting to perform the same measurements on configurations where the temperature is below the transition point, such that we are still in the broken phase. Work in this direction is in progress.

Finally we have investigated the situation with different Yukawa couplings for

---

<sup>10</sup>As remarked previously a “zero” energy mode should be understood as a quasi-zero mode. The discrete approximations used in the numerical calculations imply that we have to be content with eigenvalues which get (very) close to zero.

the upper and lower components ( $h_u = 0.1$  and  $h_d = 0.25$ ). In this case the Dirac Hamiltonian ceases to be charge conjugation symmetric, and as discussed in sec. 3 we expect states which were previously degenerate to split into two states of different energy. To test this we calculated the inner product  $\langle \Psi_i | \eta_4 \tau_2 \Psi_j^* \rangle$ , where  $i$  and  $j$  denote the two eigenmodes of nearly equal energy. According to the symmetries (38), (39), the previously degenerate eigenmodes would have been related as  $\Psi_j \equiv \eta_4 \tau_2 \Psi_i^*$  in the limit  $h_u = h_d$ . As expected, we find the inner product to be close to unity for all such pairs.

## 7 Discussion

The purpose of this work has been to establish the possibility to investigate in detail by numerical methods a number of questions related to sphaleron-like transitions in the early universe. By simulations we have generated conditions which should have some resemblance with the conditions near the electroweak phase transition: a small expectation value of  $|\varphi|^2$  (compared to the tree-value determined from the Lagrange function), but the temperature still not so high that it completely masks the transitions between neighboring vacua. We are here in the lucky situation that we can use our finite lattice volume in a constructive way. Had we been working at infinite or very large volume  $V$  it is clear that the temperature fluctuations in globally defined quantities like the Chern-Simons number would be very large since they essentially grow with the square root of the volume. By fine tuning the volume and the coupling constants we can work at high temperature and corresponding small expectation values of  $|\varphi|^2$ , but still have an acceptably small change in the Chern-Simons number. The risk is that finite volume artifacts will be present, and certainly we would have to check this aspect carefully if we attempted to measure actual transition rates. Then one would have to make sure that the transition rate grew correctly with volume. In this study we have concentrated on the qualitative aspects of the individual transitions: is there any trace of topology left in the high temperature phase above the electroweak transition and can it be associated with level crossing in the usual way?

We have seen that the gauge fields indeed behave like continuum configurations with respect to change of Chern-Simons number and level crossing and chirality of the massless fermions. As mentioned in the introduction it is not a priori clear how this picture survives the coupling to the Higgs sector of the electroweak theory. However, for not too large values of the Yukawa coupling  $h_y$  ( $h_y \leq 0.5$ ) we have observed the diving of a single eigenvalue to zero and an associated flip in the generalized chirality  $\tilde{\Gamma}_5$  when the Chern-Simons number changes by one unit. The



natural interpretation of this is that energy eigenvalues of eigenmodes of opposite generalized chirality cross at zero energy. The crossing is not linked in any precise way to the point where  $\Delta N_{CS} = 1/2$ , but as discussed in sec. 4 one would not expect this for general gauge-Higgs configurations<sup>11</sup>. The observed picture of level crossing and especially chirality flip is enhanced by stripping off the high energy thermal fluctuations of the gauge and the Higgs fields. This is an indication that the low frequency part of the Higgs field indeed has some topological content, even if it is clear that the Higgs configurations from the outset are rather “wild”. It also shows that we presumably have a “renormalization” of the chirality due to fluctuations, as mentioned in sec. 3. The break down of any sensible eigenvalue flow and chirality flip for  $h_y \geq 1$  is probably due to the fluctuations of the radial part of the Higgs field. In sec. 4 where the radial part of the Higgs field was smooth we could choose a considerably larger  $h_y$  before we encountered any problems with eigenvalues and chirality. When we use the relaxation algorithm on the configuration the situation does not improve much. On the other hand we know from direct measurements that the phase of the Higgs field and the gauge field are almost totally correlated after 8 relaxation steps and that we get very sensible results for smaller values of  $h_y$ . Since our relaxation algorithm works rather slowly on the radial part of the Higgs field, it is natural to expect the fluctuations of the radial part to develop into lattice artifacts for some threshold value of  $h_y$ . This threshold value should depend somewhat on the relaxation and we have observed this dependence.

Finally we wanted to use the measured flow of eigenvalues and the chirality flip to extract information about the topology of the Higgs field. The results obtained in sec. 4 made this procedure more ambiguous than desired. Before relaxation we can by direct measurement see that the phase of the Higgs field and the gauge field are rather decorrelated. After relaxation they are highly correlated. The basic picture of levelcrossing and chirality flip is not changed by relaxation for  $h_y \leq 0.5$  although it becomes much clearer. Unfortunately we have seen in sec. 4 that we can have level crossing and chirality flip even if the phase of the gauge and the Higgs field develop into different vacua. This means the the cooling itself could induce a change of the relative phase of the gauge and the Higgs field (from being in different vacuum sectors to being in the same vacuum sector) without a drastic change in the levelcrossing and chirality flip. To determine in more detail the topology associated with the Higgs field would therefore require additional independent measurements.

---

<sup>11</sup>Even for Yukawa coupling zero we are not aware of any analytic considerations which tell us that the crossing has to take place at the point where  $\Delta N_{CS} = 1/2$ . Furthermore our configurations do not interpolate between two vacuum configurations due to the finite temperature. The best we can say is that we start out in some neighborhood of a classical vacuum and end up near another classical vacuum.

**Acknowledgements** - SJH was partly supported by a CERN Fellowship and is now supported by a SERC Advanced Fellowship. KF would like to thank the CERN Theory Division for hospitality during the final phase of this work. GK thanks DESY and NBI for their warm hospitality. JA and GT thank the Danish Research Council for a grant which made it possible to run part of the simulations on the UNI-C CM-machine.

## References

- [1] G. 't Hooft, Phys. Rev. Lett. 37 (1976) 8; Phys. Rev. D14 (1976) 3432.
- [2] J. Ambjørn, T. Askgaard, H. Porter and M.E. Shaposhnikov, Phys. Lett. B244 (1990) 479; Nucl. Phys. B353 (1990) 346.
- [3] J. Ambjørn and K. Farakos, Phys. Lett. B294 (1992) 248; Nucl. Phys. B (Proc. Suppl) 30 (1993) 711.
- [4] A. Ringwald, Phys.Lett. B213 (1988) 61.
- [5] J. Boguta and J. Kunz, Phys.Lett. B154 (1985) 407.
- [6] C. Callias, Commun.Math.Phys. 62 (1978) 213.
- [7] C.G. Callan, R. Dashen and D.J. Gross, Phys. Rev. D17 (1978) 2717.
- [8] N. H. Christ, Phys.Rev. D21 (1980) 1591.
- [9] J. Kiskis, Phys.Rev. D18 (1978) 3590.
- [10] J. Kunz and Y. Brihaye, *Fermions in the background of sphaleron barrier*, preprint, January 1993.
- [11] A.A. Anselm and A.A. Johansen *Can electroweak  $\theta$ -term be observable ?*, preprint LNPI-1778.
- [12] M. Axenides, A. Johansen and H.B. Nielsen, *The level crossing phenomenon with Yukawa Interactions*, preprint NBI-HE-93-46.
- [13] I-Hsiu Lee and R.E. Shrock, Nucl.Phys. B305 (1988) 305.
- [14] T. Reisz, Z.Phys. C53 (1992) 169; A. Irbäck, P. Lacock, D. Miller, B. Petersson and T. Reisz, Nucl.Phys. B363 (1991) 34; P. Lacock, D. Miller and T. Reisz, Nucl.Phys. B369 (1992) 501.
- [15] C. Burden and A.N. Burkitt, Europhys. Lett. 3 (1987) 545.
- [16] C.P. van den Doel and J. Smit, Nucl. Phys. B228 (1983) 122.
- [17] H. Kluberg-Stern, A. Morel, O. Napoly and B. Petersson, Nucl. Phys. B220 [FS8] (1983) 447.
- [18] M.F.L. Golterman and J. Smit, Nucl. Phys. B245 (1984) 61.

- [19] J. Smit and J.C. Vink, Phys. Lett. B194 (1987) 433; Nucl. Phys. B298 (1988) 557.
- [20] S.J. Hands and M. Teper, Nucl. Phys. B347 (1990) 819.
- [21] D. Daniel and S.N. Sheard, Nucl. Phys. B302 (1988) 471.
- [22] S.J. Hands, Nucl. Phys. B329 (1990) 205.
- [23] I.M. Barbour and M. Teper, Phys.Lett. B175 (1986) 445.
- [24] E. Ilgenfritz, M. Laursen, M. Müller-Preussker, G. Schierholz and H. Schiller, Nucl.Phys. B268 (1986) 693.
- [25] M. Laursen and G. Schierholz, Z.Phys. C38 (1988) 501.
- [26] M. Axenides, A. Johansen and H.B. Nielsen, *On sphaleron deformations induced by Yukawa interactions*, preprint NBI-HE-93-75.

## Figure Captions

Figure 1: The Chern-Simons number as a function of the time  $t$  for the gauge configurations (45) with  $f(t) = t/T$ .

Figure 2: (a): The lowest eigenvalue as a function of time  $t$  for the gauge configurations (45) (case (1))  $h_y = 0, 0.5, 1.0$  and  $2.0$ . (b): The chirality  $\tilde{\Gamma}_5$  for the same values of  $h_y = 0$  as in (a).

Figure 3: (a): The lowest eigenvalue in case (2) for  $h_y = 0, 0.5, 1.0$  and  $2.0$  as a function of the time  $t$ . (b):  $\tilde{\Gamma}_5$  for the same values of  $h_y$ .

Figure 4: (a): The lowest eigenvalue in case (3) for  $h_y = 0, 0.25, 0.5, 0.75, 1.0$  and  $2.0$  as a function of the time  $t$ . (b):  $\tilde{\Gamma}_5$  for the same values of  $h_y$ .

Figure 5: (a): The lowest eigenvalue in case (4) for  $h_y = 0.1, 0.25, 0.50, 0.75, 1.0$  and  $2.0$  as a function of time  $t$ . (b):  $\tilde{\Gamma}_5$  for the same values of  $h_y$ .

Figure 6: A typical “sphaleron” transition before relaxation and after 6 relaxation steps.

Figure 7: (a): The “crossing” of the lowest eigenvalue and (b): the change in chirality for the transition shown in fig. 1.

Figure 8: (a): The lowest eigenvalue for a sequence of configurations which reach the “sphaleron peak” corresponding to  $\Delta N_{CS} = 1/2$ , and the return to configurations with  $\Delta N_{CS} = 0$ . (b): The change in chirality for the same configurations.

Figure 9: (a): The lowest eigenvalue  $\lambda_0$  of the massive Dirac equation (31) for different choices of the mass close to a sphaleron-like transition. On the figure we shown the difference  $\lambda_0 - m$  which is always positive. (b): The chirality (34) for the same configurations and masses as in (a).

Figure 10: (a): The lowest eigenvalue near a sphaleron-like transition for  $h_y = 0.1, 0.25$  and  $0.5$ . (b):  $\langle \tilde{\Gamma}_5 \rangle$  for the same configurations and same values of  $h_y$  as in (a).

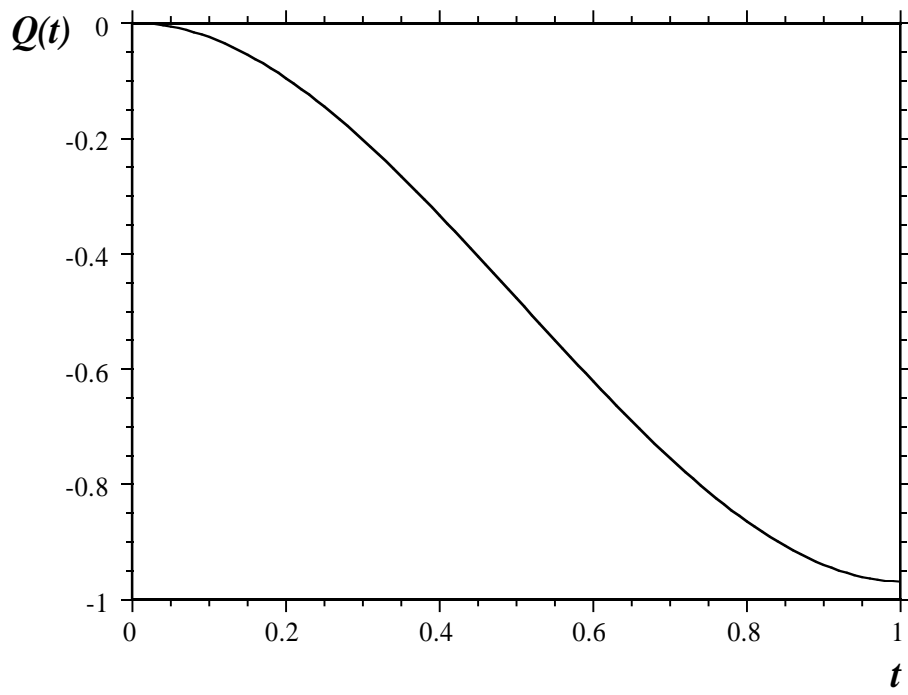
Figure 11: (a): The lowest eigenvalue for near a sphaleron-like transition for  $h_y = 0.1$  and  $0.5$ . The time  $t_0$  where the eigenvalue crosses zero has a much weaker dependence on  $h_y$  than the transition considered in fig. 10. (b):  $\langle \tilde{\Gamma}_5 \rangle$  for the same configurations and values of  $h_y$  as in (a).

Figure 12: (a)-(b): The lowest eigenvalue and  $\langle \tilde{\Gamma}_5 \rangle$  for the sphaleron-like transition used in fig. 11 for  $h_y = 0.1$ , if the configurations has undergone 0, 4 and 8 relaxations. (c)-(d): The same figures as in (a)-(b), only with  $h_y = 0.5$ .

This figure "fig1-1.png" is available in "png" format from:

<http://arxiv.org/ps/hep-lat/9401028v1>

*Fig. 1*



This figure "fig2-1.png" is available in "png" format from:

<http://arxiv.org/ps/hep-lat/9401028v1>



This figure "fig3-1.png" is available in "png" format from:

<http://arxiv.org/ps/hep-lat/9401028v1>

This figure "fig4-1.png" is available in "png" format from:

<http://arxiv.org/ps/hep-lat/9401028v1>

This figure "fig5-1.png" is available in "png" format from:

<http://arxiv.org/ps/hep-lat/9401028v1>

This figure "fig1-2.png" is available in "png" format from:

<http://arxiv.org/ps/hep-lat/9401028v1>

This figure "fig2-2.png" is available in "png" format from:

<http://arxiv.org/ps/hep-lat/9401028v1>



This figure "fig3-2.png" is available in "png" format from:

<http://arxiv.org/ps/hep-lat/9401028v1>

This figure "fig4-2.png" is available in "png" format from:

<http://arxiv.org/ps/hep-lat/9401028v1>



This figure "fig5-2.png" is available in "png" format from:

<http://arxiv.org/ps/hep-lat/9401028v1>

This figure "fig1-3.png" is available in "png" format from:

<http://arxiv.org/ps/hep-lat/9401028v1>

This figure "fig2-3.png" is available in "png" format from:

<http://arxiv.org/ps/hep-lat/9401028v1>

This figure "fig3-3.png" is available in "png" format from:

<http://arxiv.org/ps/hep-lat/9401028v1>

Fig. 3

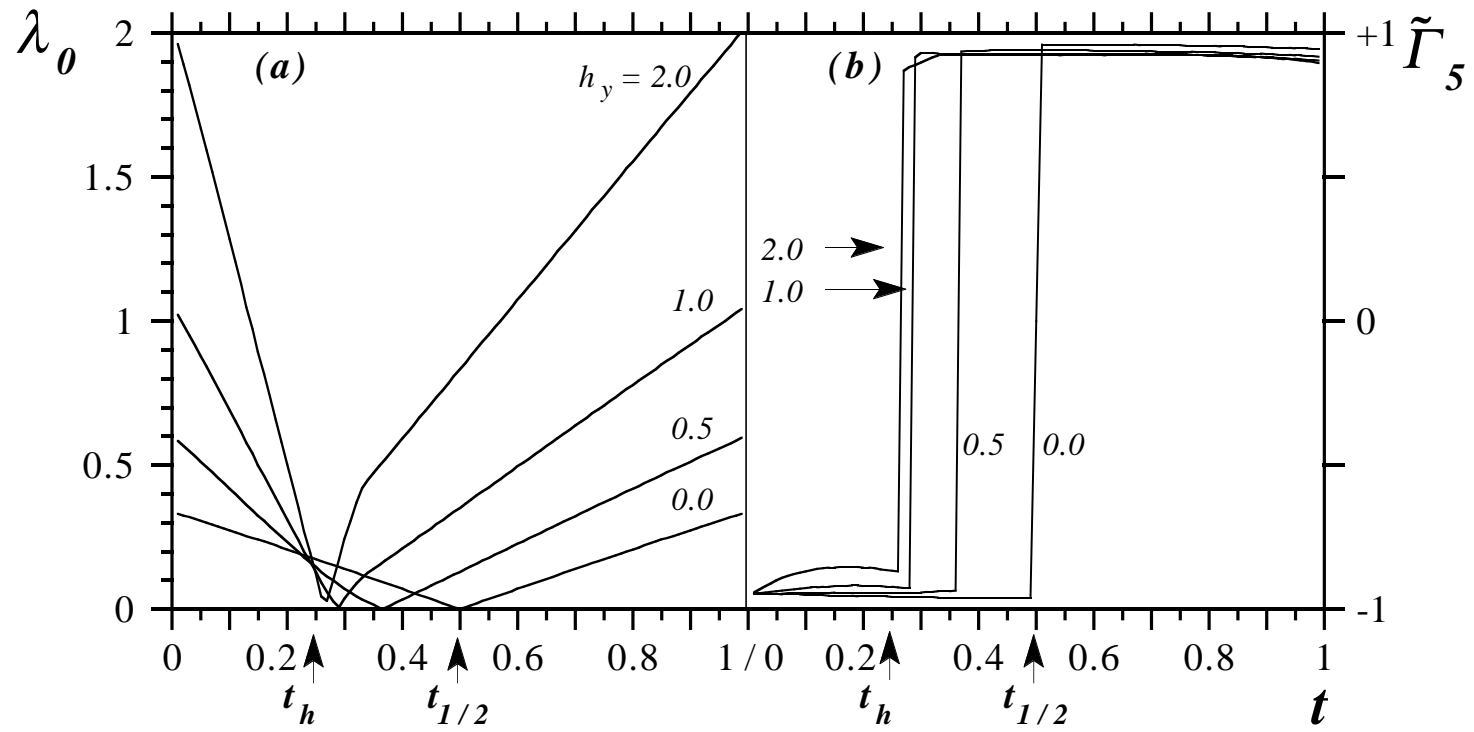


Fig. 4

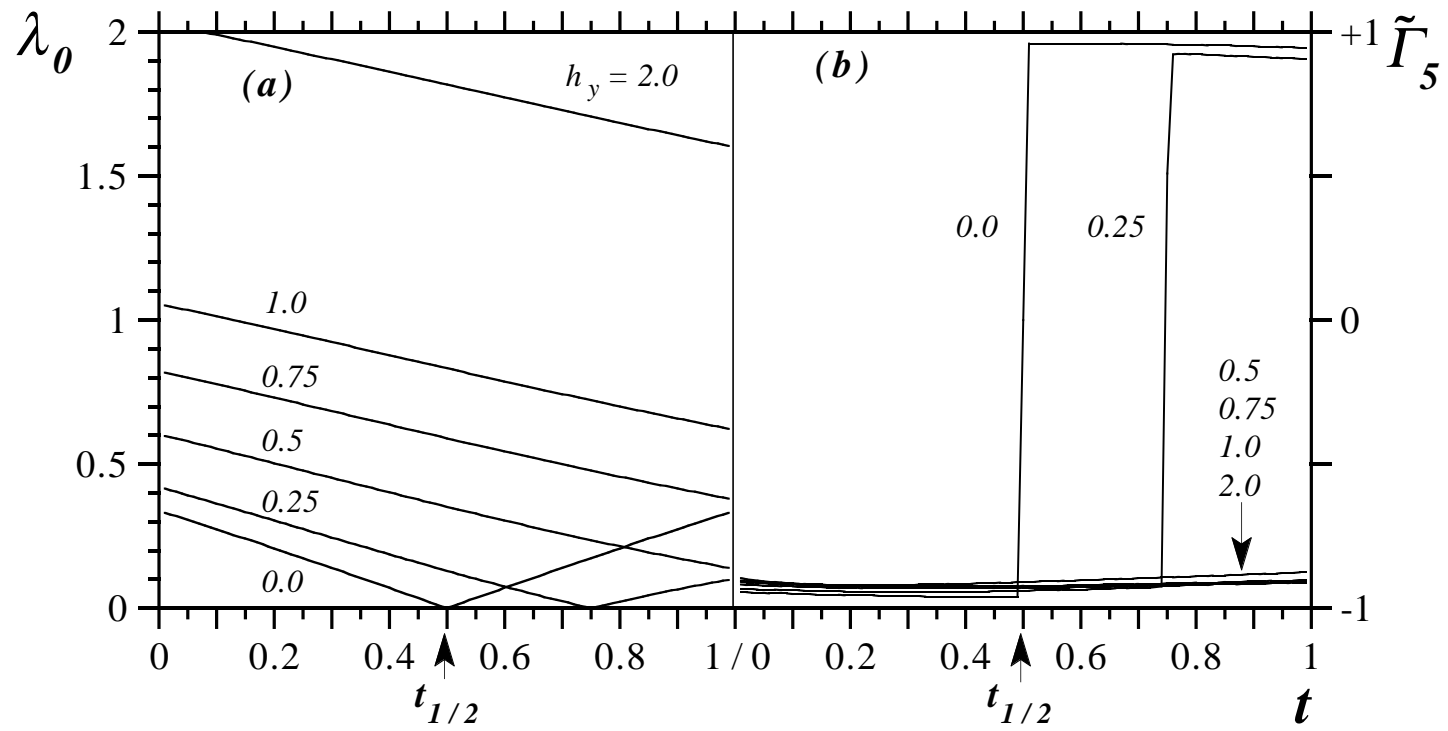
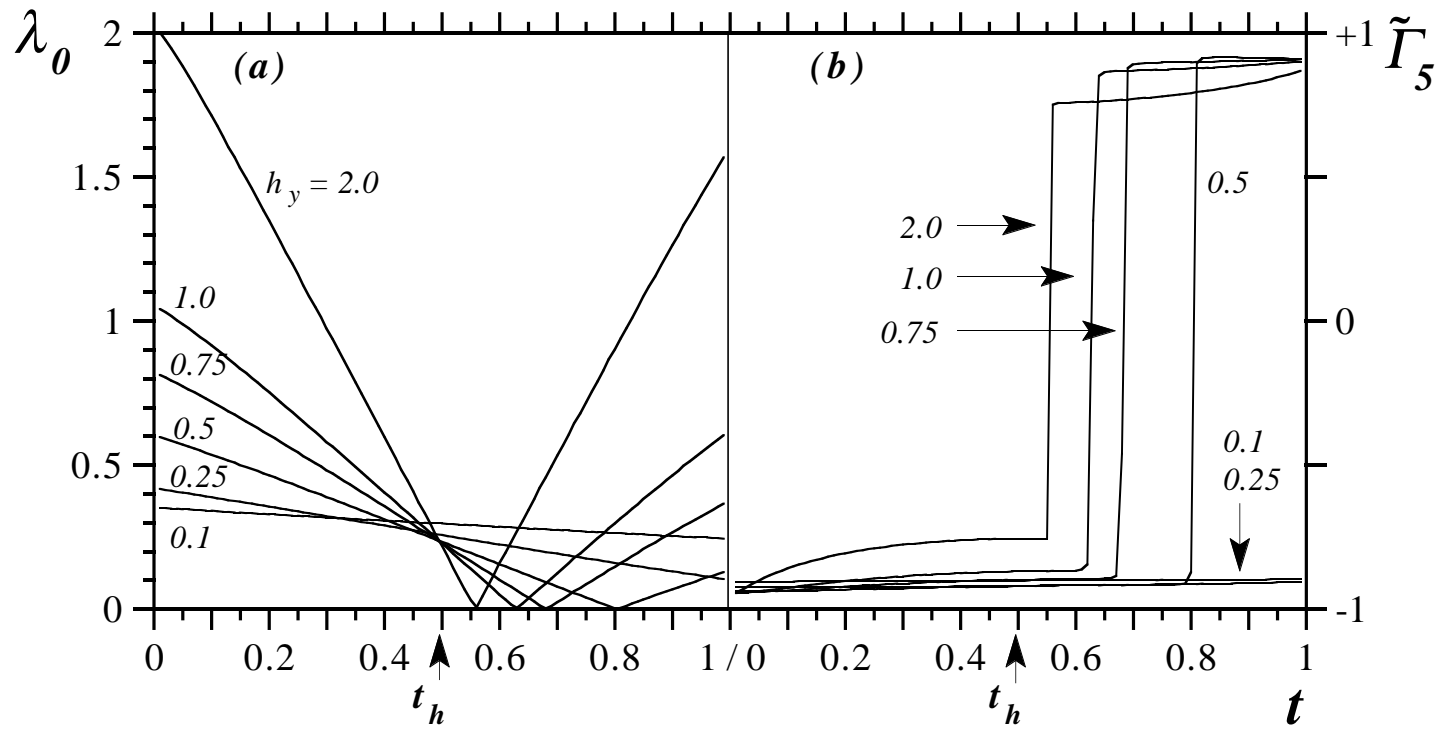


Fig. 5



*Fig. 6*

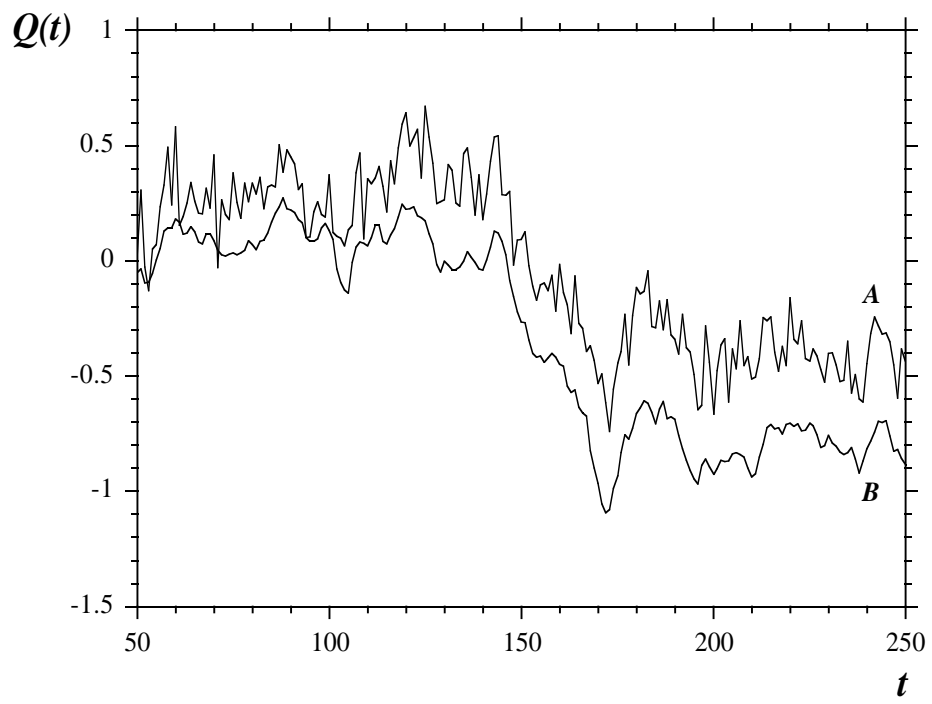




Fig. 7

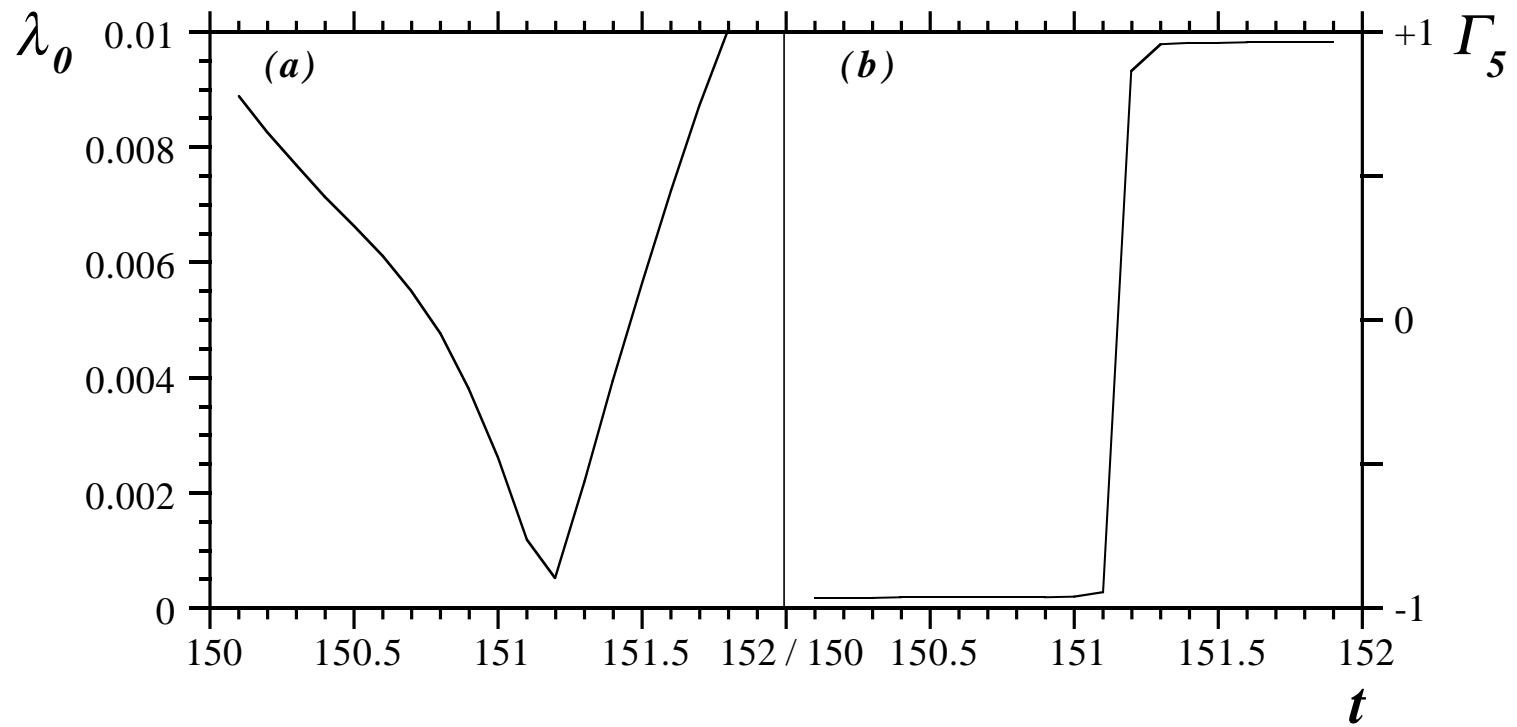


Fig. 8

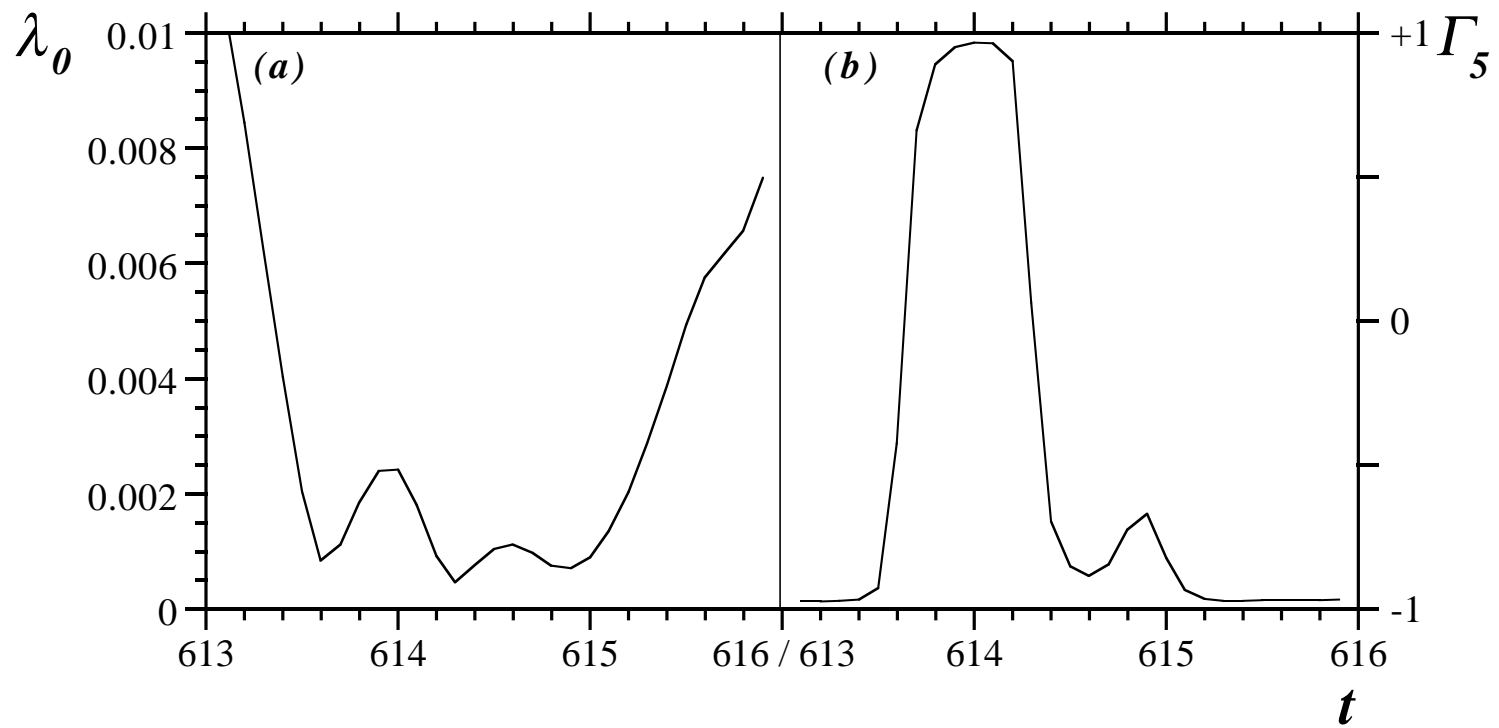


Fig. 9

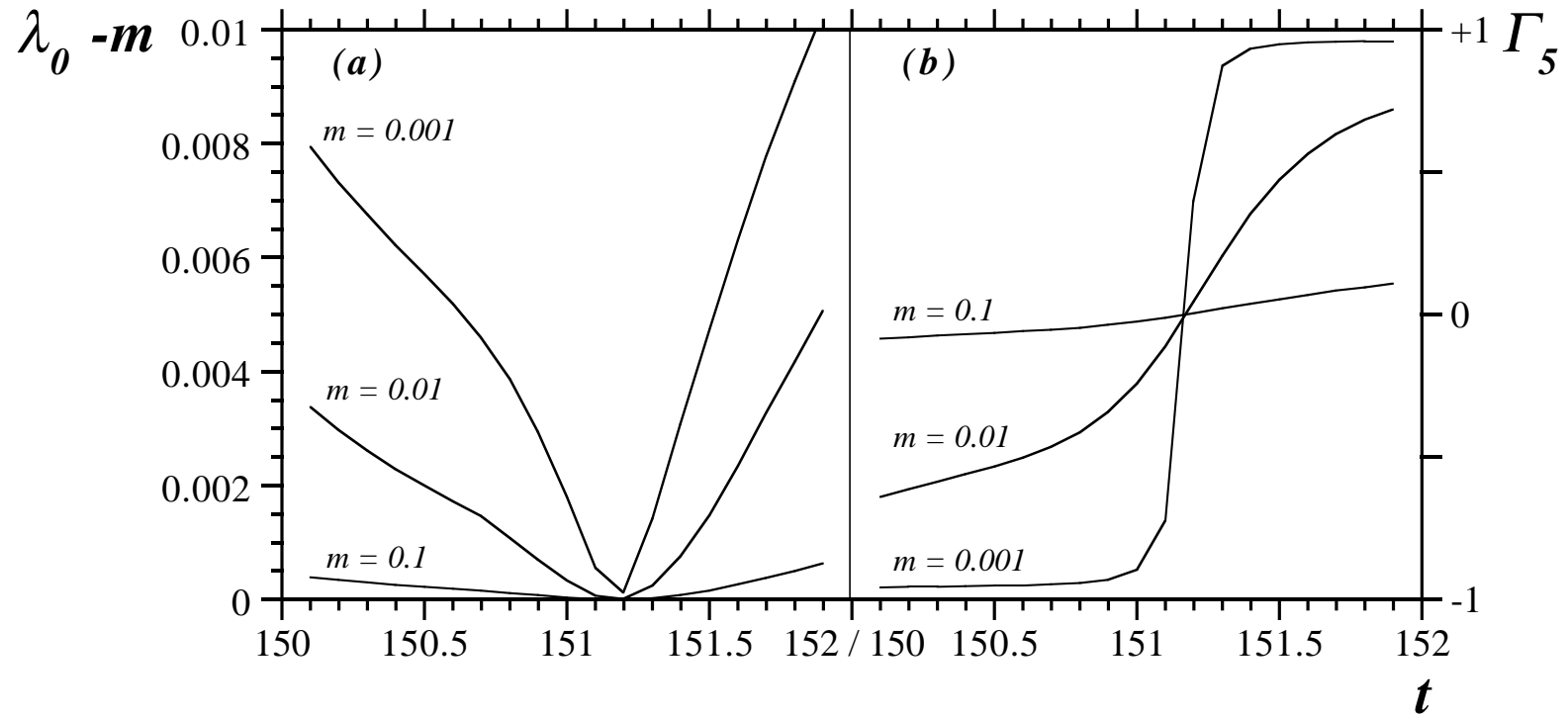


Fig. 10

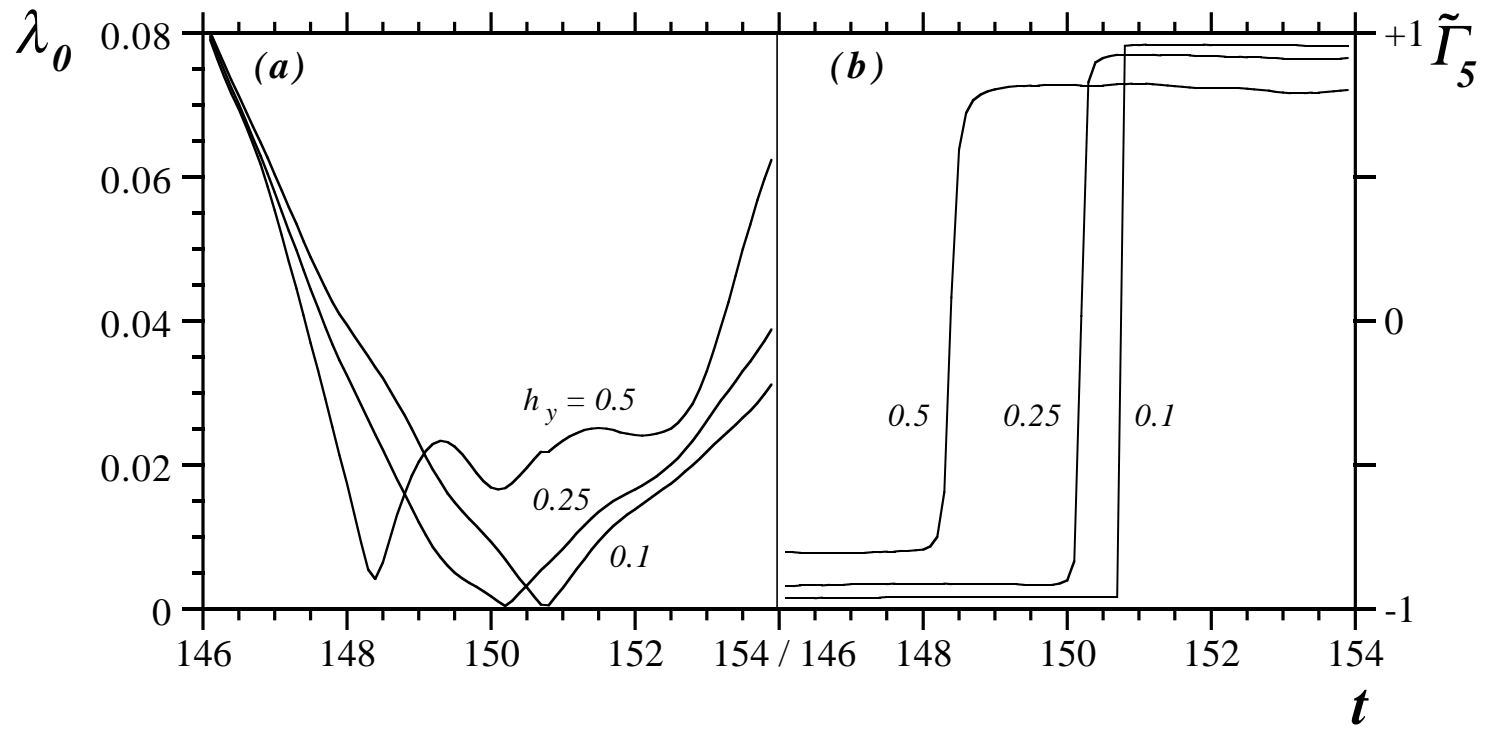


Fig. 11

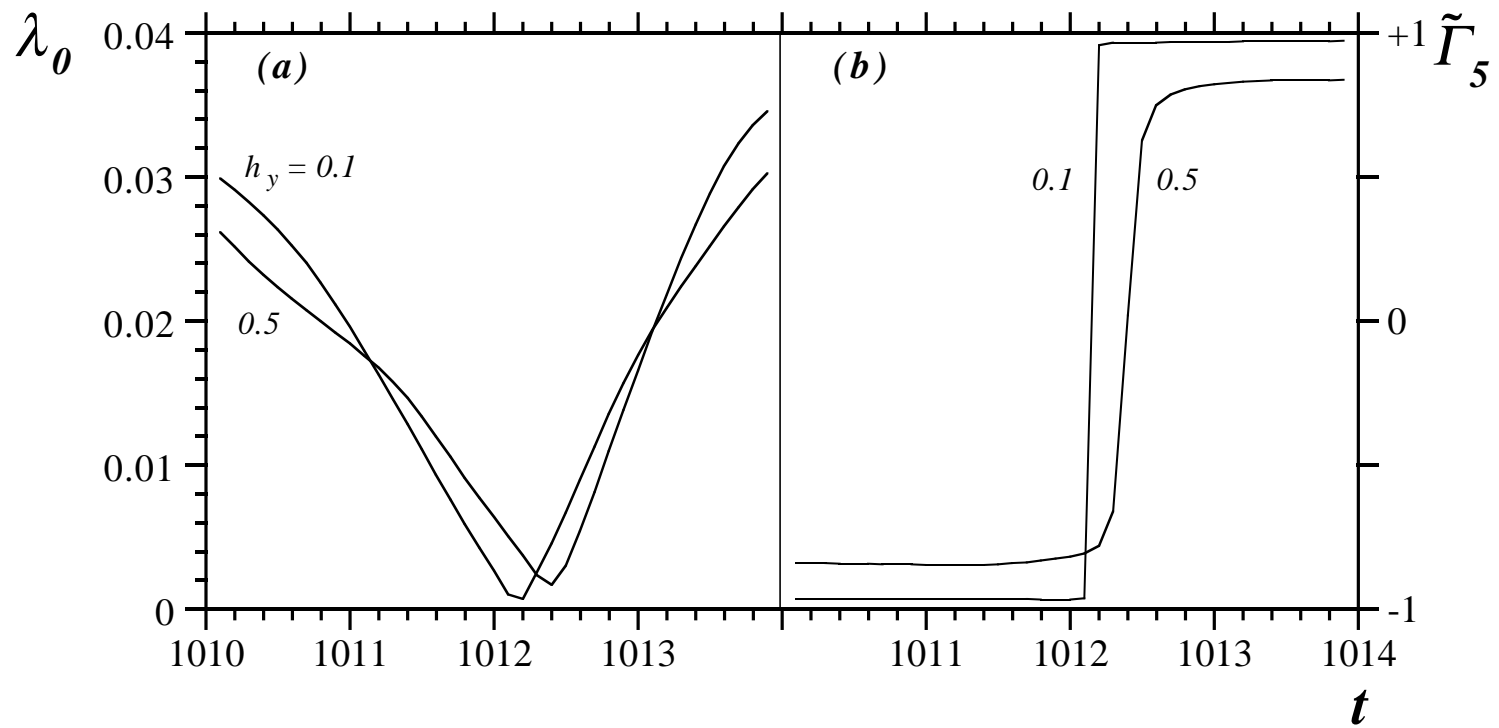


Fig. 12(ab)

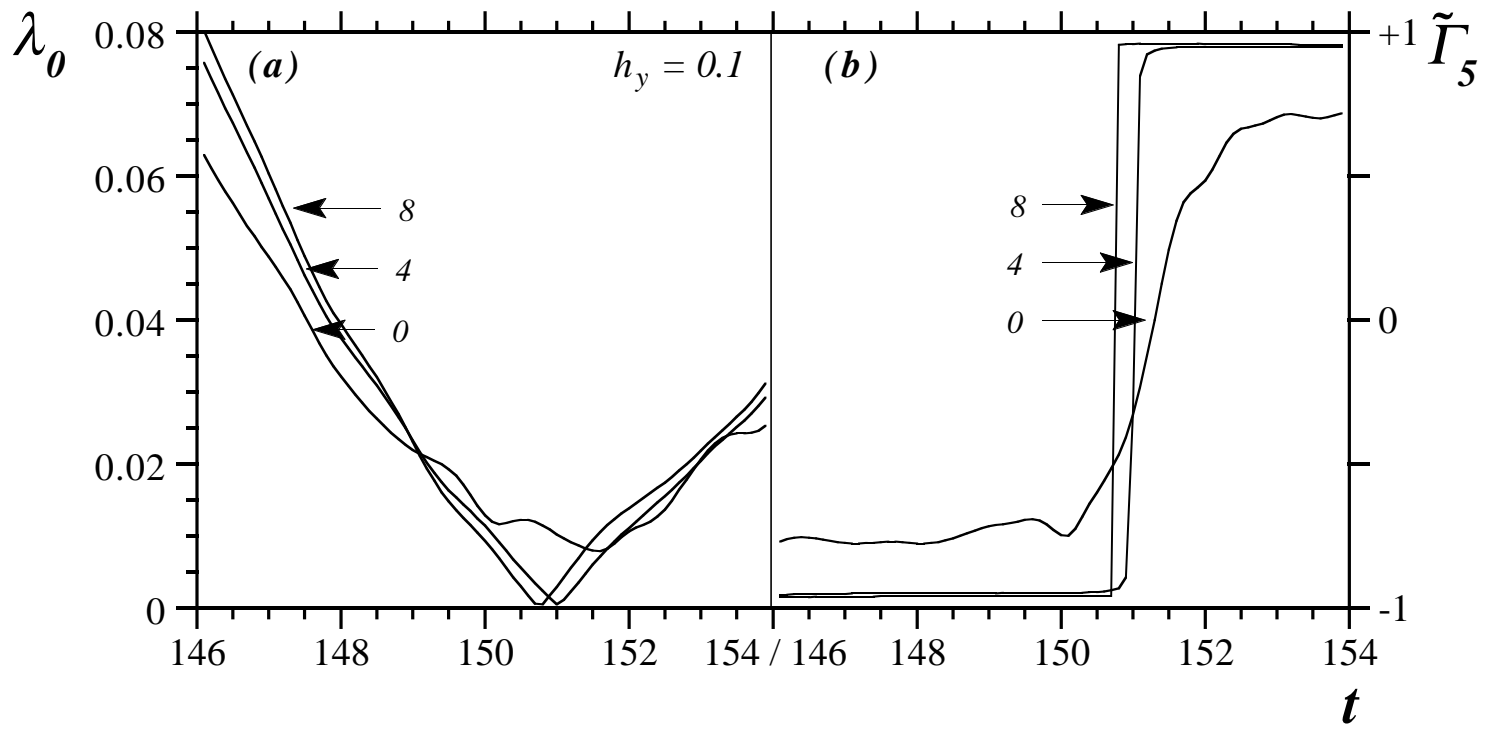


Fig. 12(cd)

